2D Seismic Imaging of the Koillismaa Layered Igneous Complex, North-Eastern Finland

Brij Singh[1], Andrzej Górszczyk[1], Michał Malinowski[1,2], Suvi Heinonen[3], Uula Autio[2], Tuomo Karinen[2], Marek Wojdyła[4], and the SEEMS DEEP Working Group*

[1]Institute of Geophysics, Polish Academy of Sciences Warsaw, Księcia Janusza 64, 01-452 Warsaw, Poland
[2]Geological Survey of Finland, Vuorimiehentie 5, 02151 Espoo, Finland
[3]Institute of Seismology, University of Helsinki, PO BOX 68 (Pietari Kalmin katu 5), Helsinki, Finland
[4]Geopartner Geofizyka Sp. z o.o., Skośna 39B, 30-383, Kraków, Poland
~~*A full list of authors appears at the end of the paper~~

Correspondence to: Brij Singh (bsingh@igf.edu.pl~~)~~), *A full list of authors appear at the end of the article

Abstract. The Seismic and Electromagnetics Methods for Deep mineral exploration (SEEMS DEEP) project is associated with the Koillismaa Layered Igneous Complex (KLIC) in north-eastern Finland. The KLIC is characterized by a Bouguer positive gravity and magnetic anomaly zone connecting the two exposed ends of the KLIC i.e. the Koillismaa intrusion and the Näränkävaara intrusion. The KLIC has the potential to host several critical raw minerals, like nickel and cobalt which are included in the European Union's critical raw material list. For this purpose, two ~~regional~~reflection seismic profiles were acquired to map the regional reflectivity in the area~~, constraining~~ with a focus on imaging the large-scale ~~information about the~~ geological architecture of the KLIC~~.~~ and the associated mineralization. Seismic imaging delineated reflectivity up to a depth of ~5 – 6 km with several distinctive reflective packages at various depths~~ which may be~~ representative of the presence of dykes, faults, and major lithological contacts present in the area. ~~Several regional faults were also imaged.~~Symmetrical orientation of several shallow reflectors indicated a systematic fracturing in the area. The ~~top of the~~deep-seated magma conduit associated with the KLIC was successfully mapped ~~with hints of fault-like events cross-cutting the intrusion~~ revealing a more complex internal structure~~ that~~, suggestive of more structural or compositional heterogeneity than was ~~earlier~~previously assumed ~~of as~~to be formed from a single lithological unit. The magma conduit is characterised as a vertically extensive mafic-ultramafic package with the potential of hosting orthomagmatic critical raw material deposits of mostly Ni-Cu-PGE sulphide type. A system of overthrust – steep regional faults was imaged for the first time in the western part of the study area. It ~~was~~is interpreted that ~~a second magma conduit~~ such steep fault systems might ~~exist between the Koillismaa intrusion~~have played a key role in magma emplacement by acting as pathways for ascending melts and ~~the Näränkävaara Intrusion.~~mineralising fluids. Results were compared against the available petrophysical data and a preliminary ~~available~~ geological model based on the density model ~~of~~from the gravity inversion with constraints from the drillhole data.

Keywords

Formatted: Font color: Text 1

Formatted: Font color: Text 1, Superscript

Formatted: Font color: Text 1 (repeated 28 times)

Land seismics; ~~curvelet; regional reflectivity;~~ Koillismaa; ~~Layered~~layered igneous intrusion; regional reflectivity; Näränkävaara intrusion

Formatted: Font color: Text 1

Formatted: Font color: Text 1

Formatted: Font color: Text 1

~~1. Introduction~~

~~The demand for raw materials has increased rapidly in recent times for various reasons: high-tech solutions, developing green energy, pushing towards a carbon-neutral society, sustainability, etc. (European Commission Report, 2023). Therefore, it is required to explore newer and deeper targets to sustain the supply and demand equilibrium. Ore deposits associated with mafic to ultramafic igneous rocks hold great potential to fulfil this requirement (Ripley and Li, 2018). The Koillismaa Layered Intrusion Complex has been of interest among geologists for several decades due to its potential to host critical raw materials (Alapieti, 1982; Karinen, 2010). The rocks of similar lithologies worldwide were found to be rich in Ni-Cu-Co-PGE and Cr-V-Ti-Fe type deposits (Barnes et al., 2016; Schulz et al., 2014). Many of these minerals like nickel, copper, cobalt, lithium, titanium metal, vanadium, etc., are in the European Union's strategic raw material list (EU Critical Raw Materials Act, 2024).~~

~~The KLIC is composed of two exposed mafic-ultramafic layered intrusions i.e. Koillismaa intrusion in the west and Näränkävaara intrusion in the east (Fig. 1). These intrusions are linked by a high gravity and magnetic anomaly zone: the Koillismaa Deep Anomaly (KDA) which has been recognized since the earliest ground gravimetric and airborne geophysical measurements conducted in the 1950s (Karinen, 2010; Salmirinne and Iljina, 2003). In 2018, the Geological Survey of Finland (GTK) acquired a low-fold 2D seismic profile in the Koillismaa area delineating a weak reflectivity at ~1.3 km and a stronger reflectivity at ~3.3 km depth which was tentatively interpreted as the top and bottom of the intrusion (KOSE2018 profile, Gislason et al., 2019). In 2020, GTK's Koillismaa deep drillhole project confirmed the presence of mafic-ultramafic plutonic rocks at a depth of ~1.4 km. Petrophysical and lab studies were done on the collected core samples from the drillhole, supplemented by limited wireline-logging data (Heinonen et al., 2022; Nousiainen et al., 2022). A deep-seated magma conduit system, named Koillismaa Feeder connects the exposed intrusion of the complex i.e. Koillismaa Intrusion and Näränkävaara Intrusion was inferred (Karinen et al., 2021b; Tirronniemi et al., 2024). This makes KLIC an interesting area to be studied in greater detail.~~

~~Geophysical surveys for mineral exploration have been routinely accomplished by potential field methods, electromagnetics, electrical methods, etc., but they lack higher resolution at deeper depths required to distinguish different lithologies. In comparison, seismic reflection surveys can provide higher-resolution images of the subsurface and have now emerged as an established method for deep mineral exploration in the hardrock environment (also called crystalline environment) (Malehmir et al., 2012). Three-dimensional (3D) surveys are often conducted for detailed mapping of the mineralization, whereas two-dimensional (2D) surveys are an excellent choice for affordable regional assessment (Bellefleur et al., 2015; Cheraghi et al., 2020; Milkereit et al., 2000; Nedimović and West, 2003 and references therein). 2D surveys also serve as a good instrument~~

~~for the initial seismic assessment of the area and can form a basis for the development of a full-scale 3D survey. It is cheaper, faster, and logistically simpler than 3D surveys (Malehmir et al., 2017; Markovic et al., 2020), but one has to be careful when interpreting 2D profiles crossing complex 3D geology.~~

~~With this aim, the Seismic and Electromagnetics Methods for Deep mineral exploration (SEEMS DEEP) project (2022–2025) was funded under the ERA-MIN 3 consortium to study the underlying geological setting of KLIC in greater detail using an integrated approach of seismics and electromagnetic methods (Autio et al., 2024). Apart from being a method-development playground, the project aims to improve our understanding of the geology of the Koillismaa area. Two regional crooked 2D reflection seismic profiles were acquired along with a 3D seismic survey (see details in Malinowski et al., 2024) in August 2023 in the vicinity of the Koillismaa drillhole. In this article, we are focusing on the results obtained from the 2D seismic profiles. Our main objective is to map the regional reflectivity in the area, supported by the petrophysical data, and to constrain the first-order geometry of the unexposed part of KLIC.~~

1. Introduction

The demand for raw materials has increased rapidly in recent times for various reasons: high-tech solutions, developing green energy, push towards a carbon-neutral society, sustainability, etc. (European Commission, 2023). As a result, there is a growing need to explore new and deeper targets to maintain the balance between supply and demand. Ore deposits associated with mafic to ultramafic igneous rocks hold great potential to fulfil this requirement, e.g., sulphide deposits, chromite deposits, carbon mineralization, etc. (Ripley and Li, 2018). The Koillismaa Layered Intrusion Complex (KLIC) has been of interest among geologists for several decades due to its potential to host critical raw materials (Alapieti, 1982; Karinen, 2010). The rocks of similar lithologies worldwide were found to be rich in Ni-Cu-Co-PGE and Cr-V-Ti-Fe type deposits (Barnes et al., 2016; Schulz et al., 2014). Many of the associated elements, such as nickel, copper, cobalt, lithium, titanium, vanadium, etc., are in the European Union's strategic raw material list (EU Critical Raw Materials Act, 2024).

The KLIC is composed of two exposed mafic-ultramafic layered intrusions, i.e. the Koillismaa intrusion in the west and the Näränkävaara intrusion in the east (Fig. 1). These intrusions are linked by a high gravity and magnetic anomaly zone: the Koillismaa Deep Anomaly (KDA), which has been recognized since the earliest ground gravimetric and airborne geophysical measurements conducted in the 1950s (Karinen, 2010; Salmirinne and Iljina, 2003). In 2018, the Geological Survey of Finland (GTK) acquired a low-fold 2D seismic profile in the Koillismaa area delineating a weak reflectivity at ~1.3 km and a stronger reflectivity at ~3.3 km depth which was tentatively interpreted as the top and bottom of the intrusion (Fig. 2, KOSE2018 profile, Gislason et al., 2019). In 2020, GTK's Koillismaa deep drillhole project confirmed the presence of the mafic-ultramafic plutonic rocks at a depth of ~1.4 km from the surface. A deep-seated magma conduit system which connects the exposed intrusion of the complex, i.e. the Koillismaa Intrusion and the Näränkävaara Intrusion were inferred (Karinen et al., 2021b; Tirronniemi et al., 2024). This makes KLIC an interesting area to be studied in greater detail.

Geophysical surveys for mineral exploration have been routinely accomplished by potential field methods, electromagnetics, electrical methods, etc. but they lack higher resolution at deeper depths required to distinguish different lithologies. In comparison, seismic reflection surveys can provide higher-resolution images of the subsurface and have now emerged as an established method for deep mineral exploration in the hardrock environment (also called crystalline environment) (Malehmir et al., 2012). In this regard, three-dimensional (3D) surveys are often conducted for detailed mapping of the mineralization, whereas two-dimensional (2D) surveys are an excellent choice for affordable regional assessment (Bellefleur et al., 2015; Cheraghi et al., 2020; Milkereit et al., 2000; Nedimović and West, 2003 and references therein). 2D surveys are also valuable for the initial seismic assessment of the area and can form a basis for the development of a full-scale 3D survey. 2D surveys are cheaper, faster, and logistically simpler than 3D surveys (Malehmir et al., 2017; Markovic et al., 2020), but one has to be careful when interpreting 2D profiles crossing complex 3D geology.

SEEMS DEEP project (2022–2025) was funded under the ERA-MIN 3 consortium to study the underlying geological setting of KLIC in greater detail using an integrated approach of seismics and electromagnetic methods (Autio et al., 2024). Apart from being a method-development playground, the project aims to improve our understanding of the geology of the Koillismaa area. Within this aim, two regional crooked 2D reflection seismic profiles were acquired in August 2023 in the vicinity of the Koillismaa drillhole along with a 3D seismic survey (see details in Malinowski et al., 2024). The main objectives of the 2D seismic survey was: (i) mapping of the regional reflectivity in the area, (ii) imaging of the large-scale geometrical architecture of the magma conduit associated with the KLIC, (iii) to obtain a first-order information on the mineralization potential of KLIC, and (iv) to provide a constrain on the geometrical nature of the KLIC beyond the coverage of the 3D survey. In this article, we will discuss the results for the first three objectives supported by the petrophysical data and the a priori geological model available in the study area.

2. Geology of the area, previous geophysical studies, and petrophysical analysis

Formatted: Font color: Text 1

Formatted: Font color: Text 1

~~The Fennoscandian Shield hosts numerous ~2.51–2.43 Ga mafic-ultramafic layered intrusions which were formed during the magmatism that led to the breakup of one or more Archaean cratons (Bleeker and Ernst, 2006; Ciborowski et al., 2015; Heaman, 1997; Köykkä et al., 2022; Skyttä et al., 2019). The Fennoscandian mafic-ultramafic intrusions are regarded as very prospective for hosting mineralization associated with critical raw materials. The ~2.44 Ga KLIC as part of the Fennoscandian Shield is a ~50 – 60 km long mafic-ultramafic layered intrusion in north-eastern Finland (Karinen, 2010). The two exposed intrusions of KLIC i.e. the Koillismaa Intrusion and the Näränkävaara Intrusion (Fig. 1), are linked by a ~50 km long positive gravity and magnetic anomaly (Karinen, 2010; Salmirinne and Iljina, 2003). Previous interpretations of the observed Bouguer~~

~~anomaly suggested a mafic dyke-like intrusion (magma conduit) of about ~2.5 – 4 km in width, and the depth from the top at ~1 – 2 km (see Fig. 1a) (Salmirinne and Iljina, 2003).~~

~~GTK acquired a low-fold 2D seismic profile in the KDA area in 2018 as a part of the siting study before the deep research drilling project. The seismic survey profile named KOSE2018 (Fig. 2), delineated the top of the intrusion at ~1.3 km as a weak reflector and the bottom at ~3.3 km depth with stronger reflectivity (Gislason et al., 2019). In 2020–2021, a diamond drillhole next to the survey profile (red star in Fig. 1, drillhole shown in Fig. 2 and Fig. 3) confirming the presence of the ultramafic rocks at a depth of more than ~1.4 km (Karinen et al., 2021b; Tirronniemi et al., 2024), thus verifying the presence of a deep-seated magma conduit system connecting the exposed intrusions of the complex (Karinen et al., 2021a). Extensive petrophysical and lab studies were performed on the collected drill core samples and classifications were made of different lithologies and rock types (Heinonen et al., 2022; Nousiainen et al., 2022). As per these studies, the surface bedrock geology at the Koillismaa study site is mainly composed of homogenous orthogneisses, cross-cutting diabase dykes, and a narrow belt of banded iron formations. The magma conduit at the depth is characterized by the mafic-ultramafic rocks such as peridotites, pyroxenites, and gabbronorites.~~

The Fennoscandian Shield hosts numerous ~2.51–2.43 Ga mafic-ultramafic layered intrusions which were formed during the magmatism associated with an extensional phase that led to the breakup of Archaean cratons (Bleeker and Ernst, 2006; Ciborowski et al., 2015; Heaman, 1997; Köykkä et al., 2022; Skyttä et al., 2019). In Finland, the ~2.44 Ga Tornio–Näränkävaara Belt (TNB; Alapieti and Lahtinen, 2002), representing the ~2.51-2.43 Ga intrusions is considered of high economic interest with a continuous history of mineral exploration and mining from much of the 20th century to the present day. The TNB is located along the contact zone between the basement and the overlying Palaeoproterozoic greenstone and schist belts extending from the Finnish–Swedish border to the Finnish–Russian border. The KLIC belongs to the TNB, and it is composed of two exposed intrusions, the Koillismaa intrusion in the west and the Näränkävaara Intrusion in the east (Fig. 1). The Koillismaa intrusion was emplaced into the boundary between the Archaean basement and the overlying Kuusamo Schist Belt (KSB) (top-left corner, Fig. 1a; Köykkä et al., 2022). The intrusion is composed of mafic-ultramafic cumulates and was later tectonically dismembered into distinct blocks which are now mostly oriented in an E–W direction (Karinen, 2010). The Näränkävaara intrusion is surrounded by the Archean gneiss and has largely retained its original position. The intrusion is mostly composed of ultramafic cumulates (Järvinen et al., 2020). These two exposed intrusions are linked to each other by a ~50 km long positive gravity and magnetic anomaly (Karinen, 2010; Salmirinne and Iljina, 2003). Previous interpretations of the observed Bouguer anomaly suggested a tubular/funnel-shaped intrusion (magma conduit) of about ~2.5 – 4 km in width, and the depth from the top at ~1 – 2 km (Salmirinne and Iljina, 2003).

The study area is mostly located within the Archaean basement. The southern part of the area is characterised by a narrow belt of banded iron formations (BIFs) marked by the red arrows in Figure 1c (Makkonen, 1972). These lithologies may be related to the Archaean greenstones known east of the study area (Järvinen et al., 2023). A major NE–SW trending sinistral Oulujärvi Shear Zone (OSZ) crosscuts the study area (Fig. 1a) (Kärki and Laajoki, 1995). There is also presence of multiple diabase dykes which are likely intruded along the fractures and faults present in the study area. According to these studies, the surface bedrock geology at the Koillismaa study site is primarily composed of homogeneous orthogneisses, cross-cutting diabase dykes and a narrow belt of banded iron formations. The magma conduit at depth is characterized by the mafic-ultramafic rocks such as peridotites, pyroxenites, and gabbronorites (see Fig. 3e).

As a part of the siting study before the deep research drilling project, GTK acquired a low-fold 2D seismic profile in the KDA area in 2018. The seismic survey profile named KOSE2018 partially overlapped the profile L1000 acquired under the SEEMS DEEP project (Fig. 2). The survey delineated the top of the intrusion at ~1.3 km as a weak reflector and the bottom at ~3.3 km depth with stronger reflectivity (Gislason et al., 2019). In 2020–2021, a drillhole (c.a. ~1724 m deep from the surface) was made next to the KOSE2018 survey profile (red star in Fig. 1, drillhole shown in Fig. 2 and Fig. 3) confirming the presence of the ultramafic rocks at a depth of more than ~1.4 km (Karinen et al., 2021b; Tirronniemi et al., 2024). This verified the presence of a deep-seated magma conduit system connecting the exposed intrusions of the complex (Karinen et al., 2021a). Extensive petrophysical and lab studies were performed on the collected drill core samples and classifications were made of different lithologies and rock types (Heinonen et al., 2022; Nousiainen et al., 2022). Recent age determinations of these mafic–ultramafic lithologies have confirmed that the magma conduit represents the same ~2.44 Ga magmatic event as the Koillismaa and Näränkävaara intrusions (Karinen et al., 2025).

A plot of P-wave velocity, density, reflection coefficient series~~,~~ and the corresponding synthetic seismogram ~~are~~is shown in Figure 3(a-d). The synthetic seismogram is produced ~~using~~by convolving the ~~Ricker wavelet~~reflection coefficients with ~~a~~the 35 Hz dominant frequency ~~of 35 Hz.~~Ricker wavelet to obtain the seismic response from the key geological units from the drillhole. A simplified lithology of the ~~borehole~~drillhole is shown in Figure 3e (red star in Fig. 1~~,~~ and Fig. 2). Average seismic P-wave velocity ranges between ~5.5 – 6.5 km/s and density between ~2800 – 3200 kg/m^3 for mafic-ultramafic rocks (~~as~~ measured on the core samples under the room temperature and pressure conditions). A clear acoustic impedance contrast was found between the ~~ultramafics~~ultramafic and the overlying felsic rocks with the presence of several cross-cutting diabase veins in the vicinity of the drill hole (see synthetic seismogram, Fig. 3d). ~~These faults/fractures and lithology changes were also~~Some of these events were imaged during the walkaway vertical seismic profiling (VSP) survey conducted in the same drillhole ~~(Malinowski et al., 2023; Tirronniemi et al., 2024).~~(Malinowski et al., 2023; Tirronniemi et al., 2024). They are marked by black arrows in Figure 3b, e.g. fault/fracture zone at ~400 m (Mylorite), the top and the bottom of the Dolerite (~550 – 650 m) and the lithology changes at c.a. 900 m (Schist (altered Diabase)). A preliminary geological model was created ~~mainly~~ based on the ~~limited surface geological data, potential field inversions, and resistivity models~~density model from ~~sparse MT stations~~the gravity inversion with constraints from the existing drillhole data.

Formatted: Font color: Text 1
Formatted: Font color: Text 1
Formatted: Font color: Text 1
Formatted: Font color: Text 1
Formatted: Font color: Text 1
Formatted: Font color: Text 1
Formatted: Font color: Text 1
Formatted: Font color: Text 1
Formatted: Font color: Text 1
Formatted: Font color: Text 1
Formatted: Font color: Text 1
Formatted: Font color: Text 1
Formatted: Font color: Text 1
Formatted: Font color: Text 1
Formatted: Font color: Text 1
Formatted: Font color: Text 1

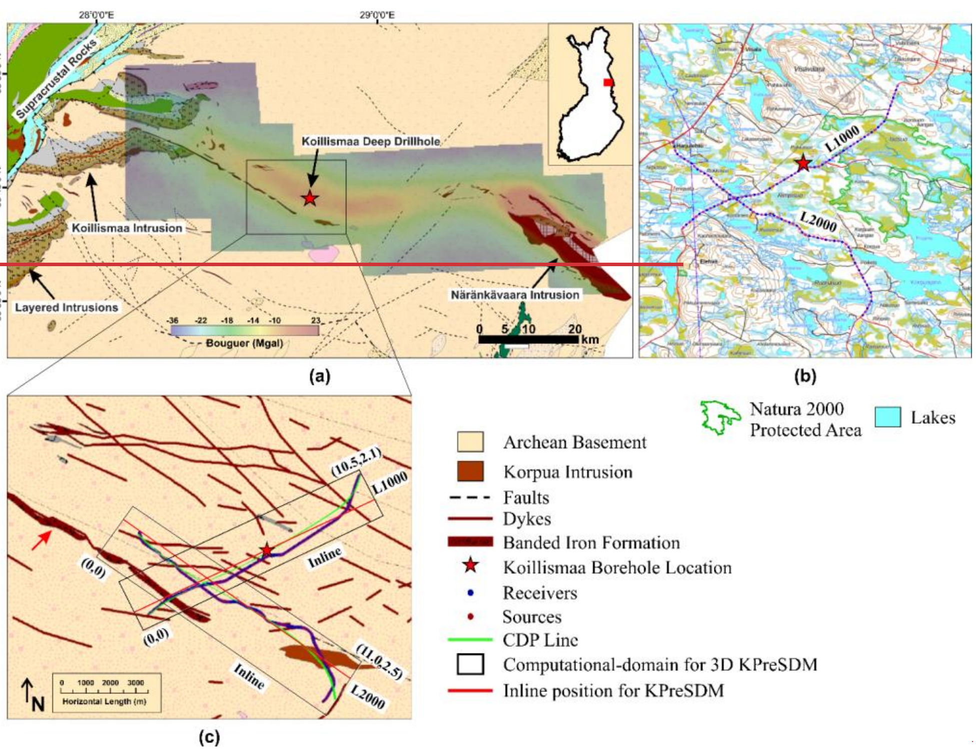
28°0'0"E
29°0'0"E
65°55'0"N
65°45'0"N
65°35'0"N
Supracrustal Rocks
Koillismaa Deep Drillhole
Koillismaa Intrusion
Layered Intrusions
Näränkävaara Intrusion
-36 -22 -18 -14 -10 23
Bouguer (Mgal)
0 5 10 20 km
(a)
L1000
L2000
(b)
(10.5,2.1)
L1000
Inline
(0,0)
(0,0)
(11.0,2.5)
Inline
L2000
N
Horizontal Length (m)
(c)
Natura 2000 Protected Area
Lakes
Archean Basement
Korpua Intrusion
Faults
Dykes
Banded Iron Formation
Koillismaa Borehole Location
Receivers
Sources
CDP Line
Computational-domain for 3D KPreSDM
Inline position for KPreSDM

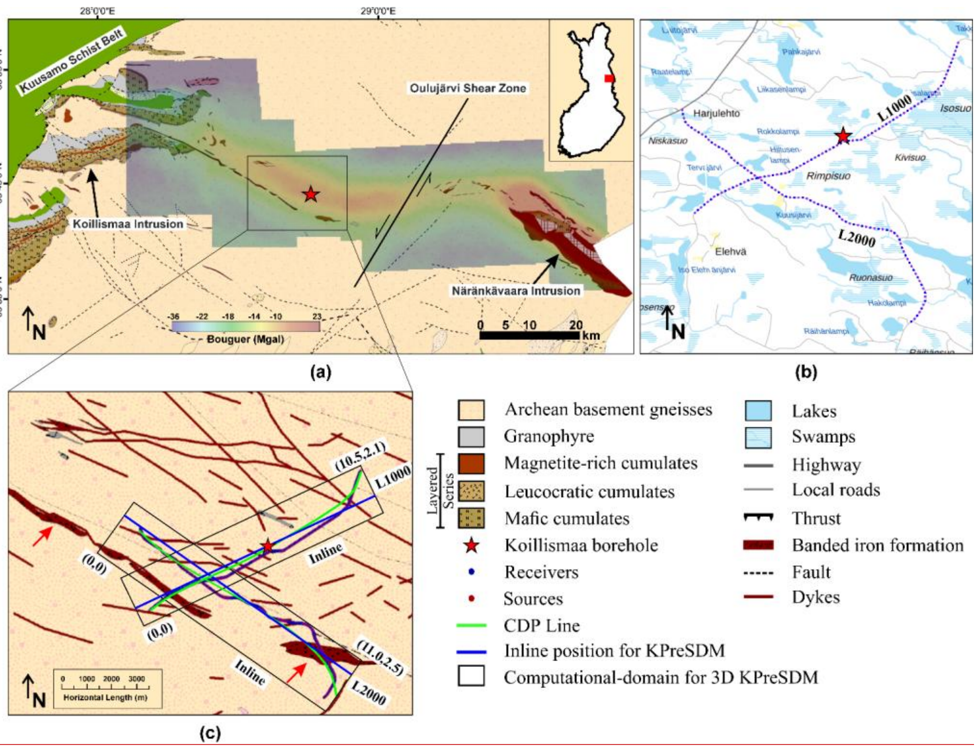

Figure 1: (a) Generalized geological map of the KLIC with the Koillismaa intrusion in the west and the Näränkävaara intrusion in the east~~.~~ (Geological map is from "Bedrock of Finland v2.3 at the scale 1:200 000", see reference). The location of the area is shown by the red rectangle over the map of Finland in the top-right inset (© Google Maps). A Bouguer gravity anomaly map is overlaid over the geological map. The red star marks the Koillismaa drillhole. (b) Seismic profiles (L1000 and L2000) overlaid on the topographic map. (c) Acquisition profiles overlaid over the geological map. Purple and blue dots mark the position of the shotpoints and receivers, respectively. The green lines show the processing lines (CDP binning line) for each profile. The black ~~box shows~~boxes show the computational domain for depth migration (in km). The ~~red~~blue line shows the position of the inline at which the results from Kirchhoff prestack depth migration (KPreSDM) are shown in Fig. 5b and 6b. Red arrows mark the banded iron formations (BIFs).

Formatted: Font color: Text 1

Formatted: Font color: Text 1

Formatted: Font color: Text 1

Formatted: Font color: Text 1

Formatted: Font color: Text 1

Formatted: Font color: Text 1

Formatted: Font color: Text 1

Formatted: Font color: Text 1

Formatted: Font color: Text 1

Formatted: Font color: Text 1

Formatted: Font: Bold, Font color: Text 1

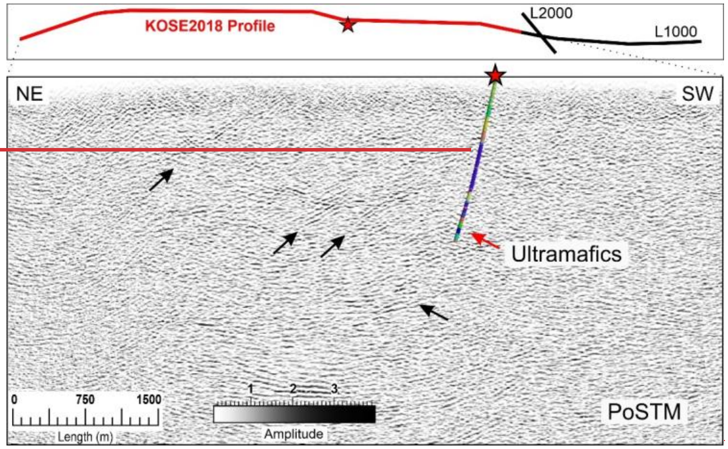

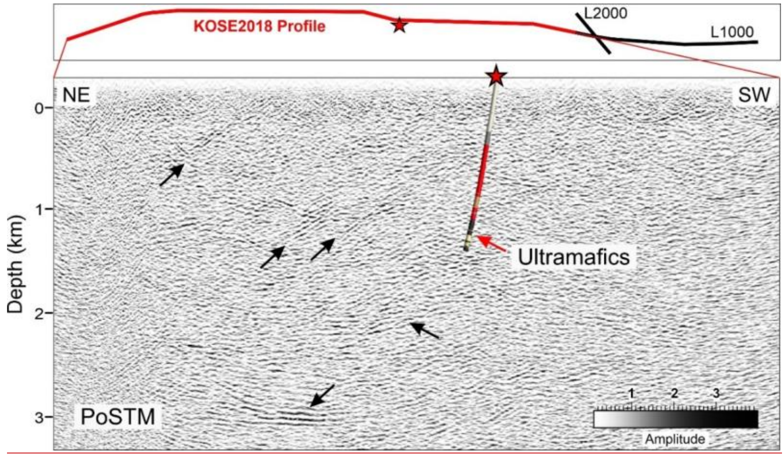

Figure 2: KOSE2018 2D seismic profile ~~(Gislason et al., 2019)~~(Gislason et al., 2019). The top panel shows the map view of the overlapping KOSE2018 profile (red) with the SEEMS DEEP profile L1000 (in black). Black arrows in the bottom panel mark different reflectors mapped in the area (compare with Fig. 5a). The ~~borehole~~drillhole is plotted for different lithologies based on the analysis of Koillismaa drill core data (red star, Fig. 1). A simplified lithology for the same is shown in Fig. 3e.

Formatted: Font color: Text 1

Formatted: Font color: Text 1

Formatted: Font color: Text 1

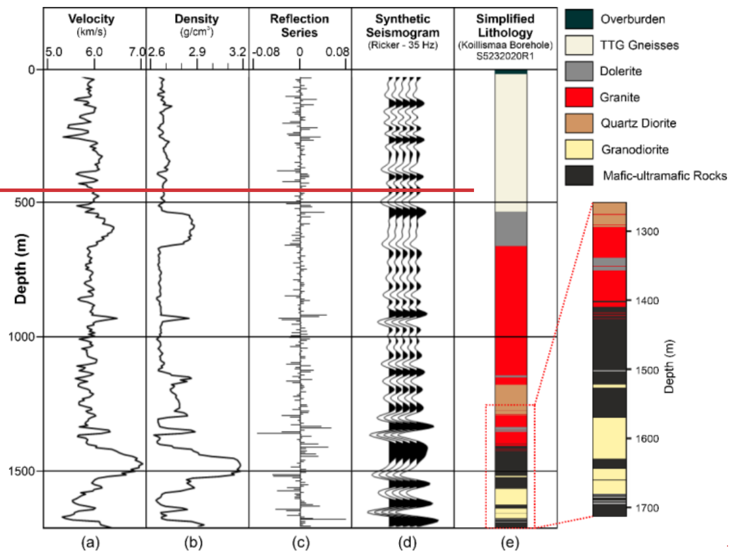
Velocity (km/s)
5.0 6.0 7.0
Density (g/cm³)
2.6 2.9 3.2
Reflection Series
-0.08 0 0.08
Synthetic Seismogram (Ricker - 35 Hz)
Simplified Lithology (Koillismaa Borehole) S5232020R1
Depth (m)
0
500
1000
1500
(a) (b) (c) (d) (e)
Overburden
TTG Gneisses
Dolerite
Granite
Quartz Diorite
Granodiorite
Mafic-ultramafic Rocks
1300
1400
1500
1600
1700
Depth (m)

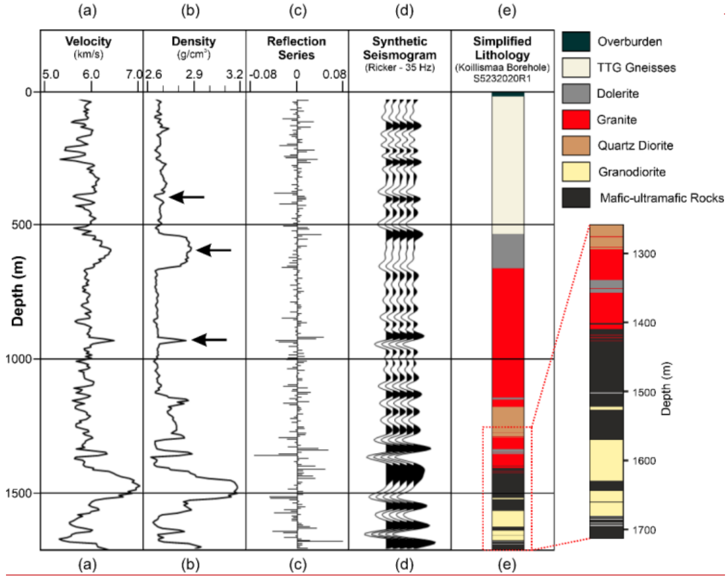
Velocity (km/s)
5.0 6.0 7.0
Density (g/cm³)
2.6 2.9 3.2
Reflection Series
-0.08 0 0.08
Synthetic Seismogram (Ricker - 35 Hz)
Simplified Lithology (Koillismaa Borehole) S5232020R1
Depth (m)
0
500
1000
1500
(a) (b) (c) (d) (e)
Overburden
TTG Gneisses
Dolerite
Granite
Quartz Diorite
Granodiorite
Mafic-ultramafic Rocks
1300
1400
1500
1600
1700
Depth (m)

Figure 3: (a), (b~~),~~) and (c) ~~Plot~~shows plot of P-wave velocity, density~~,~~ and reflection coefficient series based on the laboratory measurements on core samples from the Koillismaa drillhole (red star, Fig. 1), (d) ~~Synthetic~~synthetic seismogram produced using a Ricker wavelet with dominant frequency 35 Hz highlighting the acoustic impedance contrast between different lithologies, (e) ~~Simplified~~simplified lithology of the ~~drillhole~~drilhole (same as in Fig. 2). Drilling shows the surface bedrock geology to be composed of homogenous orthogneisses, cross-cutting dykes and the magma conduit characterized by the mafic-ultramafic rocks at an approx. ~~depth of ~1.4 km~~depth of ~1.4 km from the surface. Black arrows in Fig. 3b mark the events for which reflectivity was observed in the walkaway VSP study done in the drillhole.

3. Data Acquisition

The dataset comprises two crooked regional~~-~~ reflection seismic profiles acquired along the existing gravel roads (see map in Fig. 1b)~~.~~. The first profile, L1000, is ~10.5 km long and is oriented in the NE-SW direction roughly intersecting the ~~mafic intrusion~~KDA perpendicular to its strike ~~(see Fig. 1a and 1c)~~. The second profile, L2000, is ~11.5 km long and is oriented in the NW-SE direction (see Fig. 1a and Fig. 1c). Both profiles have a uniform receiver spacing of 15 m and shot spacing of 30 m. Blue dots mark receivers and purple dots mark shots overlapping the receiver points ~~(Fig. 1c)~~. Geospace's GS-ONE ~~Low-Frequency~~ low-frequency, three-component (GSB3-3C) land geophones with a natural frequency of 5 Hz ~~Hz~~ were used ~~with GSB3-3C recording units~~ in a continuous mode for both profiles. A 22-tonne Mark IV Vibroseis truck (48000 lbs peak force) was used as the source ~~along the existing gravel roads (see map in Fig. 1b)~~. All the acquisition parameters related to the survey are summarised in Table 1. The acquired data are of good quality with reflections visible in the raw shot gathers (Fig. 4, red arrows). The data is of better quality for shotpoints located in the southern and western end of the survey ~~for which~~where the first-break energy ~~was~~is visible for the full-offset range~~, otherwise, an effective offset of ~4 – 5 km is~~. For the remaining shotpoints, clear first breaks are generally ~~observed for the rest of the shots~~limited to approximately 4 – 5 km.

Table 1. Acquisition parameters for profiles L1000 and L2000

Data Acquisition	L1000	L2000
Spread Configuration	Fixed-spread geometry	
Receiver Spacing	15 m	
Receiver Type	3C geophone, 3C recording ~~node~~mode	
Source Spacing	30 m	
Source Type	Vibroseis (22-ton Mark IV)	
Vibroseis Sweep	20 – 160 Hz, +1dB (20-s sweep length)	
Record Length	6 s	
Number of Sweeps/Shot Point	3	
Profile Length	~10.5 km	~11.5 km
Channels	701	746
Vibroseis Source Points	348	371
Maximum CDP Fold	417	453
Elevation Changes	~246 – 268 m	~244 – 262 m

~~**4. Data Processing**~~

~~Reflection seismic data processing for both profiles followed the standard processing workflow applied to the hardrock seismics. Data preprocessing started with the extraction of the vertical component from the 3C receiver data. A crooked-line geometry was set up with rectangular bin geometry. Common Depth Point (CDP) bin spacing was kept at half of the receiver spacing sufficient to map the steeply dipping diabase veins, fault, etc. present in the area. The CDP processing line for both profiles is shown by the green line in Figure 1c. Bad traces were removed and manual picking of first-break energy for the full offset range was done for both profiles (see Fig. 4a and 4d).~~

~~**Preprocessing involved a two-layered refraction statics solution with a replacement velocity of 5 km/s to handle the heterogeneous near-surface weathering layer. A floating datum at elevation 300 m above sea level (a.s.l.)**~~**4. Data Processing**

Reflection seismic data processing for both profiles followed the standard processing workflow applied to the hardrock seismics (Cheraghi et al., 2020; Malehmir et al., 2017; Markovic et al., 2020; Nedimović and West, 2003). Data preprocessing started with the extraction of the vertical component from the 3C receiver data. A crooked-line geometry was set up with rectangular bin geometry. Common Depth Point (CDP) bin spacing was kept at half of the receiver spacing sufficient to map the steeply dipping diabase veins, fault, etc., present in the area. The CDP processing line for both profiles is shown by the green line in Figure 1c. Bad traces were removed and manual picking of first-break energy for the full offset range was done for both profiles (see Fig. 4a and 4d).

Preprocessing involved a two-layered refraction statics solution with a replacement velocity of 5 km/s to handle the heterogeneous near-surface weathering layer. A floating datum was defined to account for the ~~differences in the~~ elevation ~~of~~variations for the source and receivers. It was followed by the spherical divergence correction, automatic gain control (AGC), and deconvolution. A combination of spiking ~~deconvolution~~ and gapped deconvolution was found most effective in enhancing the data reflectivity. A notch filter was applied to remove the ~~mono-frequencies.~~monofrequencies. An airwave mute, 1D median filter~~,~~ and bandpass filter (BP) were used to attenuate the ground roll and ~~surface~~shear waves (compare Figure 4a~~,~~ with 4b, and 4d with 4e). An offset-based refraction mute ~30 ms below the first break was used. A special emphasis ~~at the pre-processing stage~~ was placed on improving the coherency of the signal of the common shot gathers with curvelet denoising ~~(Górszczyk et al., 2015)~~(Górszczyk et al., 2015) (compare Figure 4b with 4c, and 4e with 4f).

Velocities were picked on the prestack gathers resulting in the normal moveout (NMO) correction velocities in the range of ~5.7 – 6.2 km/s. However, due to the uniformity of P-wave velocity associated with homogenous geology above the target area, i.e. mafic-ultramafic rocks (~1.4 km); a constant velocity of 6 km/s ~~was found to produce~~produced similarly good results

Formatted: Font color: Text 1
Formatted: Font color: Text 1
Formatted: Font color: Text 1
Formatted: Font color: Text 1
Formatted: Font color: Text 1
Formatted: Font color: Text 1
Formatted: Font color: Text 1
Formatted: Font color: Text 1
Formatted: Font color: Text 1
Formatted: Font color: Text 1
Formatted: Font color: Text 1
Formatted: Font color: Text 1
Formatted: Font color: Text 1

when used for the NMO followed by the dip moveout correction (DMO). Final migration tests were performed for a scan of velocities in the range of ~5.0 – 6.5 km to assess the overall imaging of different geological units.

A square-root normalization stacking was done on the DMO corrected shot gathers, followed by the FX-Deconvolution and BP filtering. Stolt (~~f-k~~F-K) migration with a constant velocity of 6 km/s produced optimum results ~~aiming~~aimed at the target area. We also tested prestack time migration which produced better imaging in some areas, but overall, DMO followed by post-stack time migration (PoSTM) produced qualitatively better imaging results (i.e. with less migration artifacts). Finally, the processed time sections were converted into depth sections, and the data ~~was~~were exported for visualization. All time-domain processing parameters are summarized in Table 2.

Table 2. ~~Time-domain processing~~Processing workflow for profiles L1000 and L2000

Data ~~Preprocessing~~Preparation	
Data Extraction	vertical component
Data Read	SEG-Y, 3.0 s
Geometry Setup	crooked line, rectangular bin
Nominal CDP Spacing	7.5 m
Trace Editing	bad traces removed
First-Break Picking	manual pick
Preprocessing Stage	
Refraction Statics	2-layer model, repl. vel. – 5 km/s
~~Floating Datum~~	~~300 m a.s.l.~~
Elevation Statics	floating datum
Spherical Divergence Correction	v^2t function
AGC	250 m
Deconvolution	~~Spiking,~~spiking – 150 ms / ~~Gapped,~~gapped – 150~~ / ~~/24 ms
Notch Removal	50~~ / ~~/100 Hz
Airwave Mute	330 m/s
Linear Noise Removal	~~Median~~median filter, vel. – 2.8/3.0 km/s
Bandpass Filter (BP)	15-35-145-185 Hz
AGC	250 ms
Refraction Mute	offset-based, 30 ms below first-arrivals
Coherency Enhancement	~~Curvelet~~curvelet-denoising
NMO	~~const. velocity~~vel. – 6 km/s
Dip Moveout	~~const. velocity~~vel. – 6 km/s
Stacking and Migration	
Stacking	~~SQRT Normalization~~
FX-Deconvolution	sqrt normalization

Final Datum	11 traces (100~~-~~/30 ms window)
Migration	300 m a.s.l.
BP	Stolt (6 km/s)
	15-35-145-185 Hz
Time-to-depth Conversion	~~Vel~~vel. – 6 km/s
Data Export	~~SEGY~~SEG-Y format

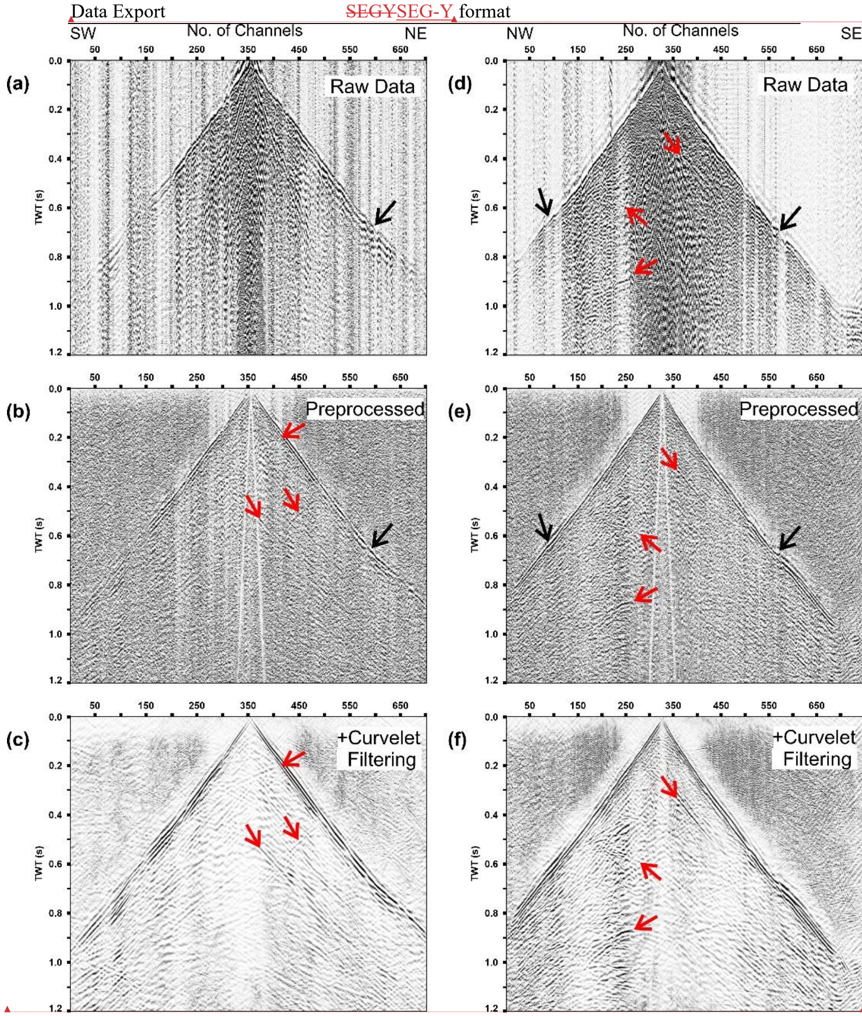

Formatted: Font color: Text 1

Formatted: Font color: Text 1

Formatted: Font color: Text 1

Formatted: Font color: Text 1

Formatted: Font color: Text 1

Formatted: Font color: Text 1

Formatted: Font color: Text 1

Formatted: Font color: Text 1

Figure 4: Result of the data preprocessing applied to profiles L1000 and L2000. (a) Raw shot gather for profile L1000, (b) data with full preprocessing without the top-mute, and (c) is the same as (b) with curvelet filtering. Trace balancing was applied for presentation purposes. (d), (e) and (f) are the same as (a), (b) and (c) for profile L2000. Black arrows show the correction of first arrivals due to the ~~heterogenous~~heterogeneous near-surface weathered layer. Red arrows mark the comparative enhancement/preservation of reflectivity in the raw shot gathers.

Formatted: Font color: Text 1
Formatted: Font color: Text 1
Formatted: Font color: Text 1
Formatted: Font color: Text 1

4.1 Depth-domain imaging

Along with PoSTM, we also tested Kirchhoff prestack depth migration (KPreSDM) due to its ability to better handle the complexity of the medium. To avoid the artifacts arising from a strict 2D migration of a crooked line, we performed KPreSDM in 3D mode ~~(Singh and Malinowski, 2022, 2023). We used the migration code of Hloušek et al. (2015) working in the shot-domain. The computational domain for KPreSDM is shown as black boxes in Figure 1c. Depth migration parameters were kept similar for both profiles given the same acquisition setup and underlying geology in the area. For profiles L1000 and L2000, the grid dimensions are 701 x 141 x 434 and 735 x 168 x 434 (inline x crossline x depth) with a uniform grid spacing of 15 m. Similarly to PoSTM, a migration velocity of 6 km/s was used, however, KPreSDM was also tested for a scan of velocities in the range of ~5 – 6.5 km/s.~~ (Singh and Malinowski, 2022, 2023). We used the migration code of Hloušek et al. (2015) in the shot-domain. The computational domain for KPreSDM is shown as black boxes in Figure 1c. Depth migration parameters were kept similar for both profiles, given the same acquisition setup and underlying geology in the area. For profiles L1000 and L2000, the grid dimensions were 701 x 141 x 434 and 735 x 168 x 434 (inline x crossline x depth) with a uniform grid spacing of 15 m. Similarly to PoSTM, a migration velocity of 6 km/s was used; however, KPreSDM was also tested for a scan of velocities in the range of ~5 – 6.5 km/s. No additional processing was applied to the dataset used for KPreSDM.

Formatted: Font color: Text 1

5. Results

Processing and time/depth imaging of the seismic data resulted in portraying several reflective packages at various depths~~ of the subsurface.~~. Figure 5 shows imaging results for profile L1000. Figure 5a shows the standard DMO-PoSTM ~~sections~~section. The origin (zero depth) is at 300 m a.s.l. and is the same for all the results presented in this article. Reflections are imaged down to a depth range of ~5 – 6 km~~ are imaged~~. Events are less focussed in the first kilometre, although there are hints of steep reflectors projecting towards the surface (see black arrows labelled SF1-SF4). Other prominent reflections imaged at various depths are also marked by the black arrows. ~~Arcuate~~An arcuate reflectivity is mapped in the central area of the profile (~~marked by~~ blue arrows). ~~Its top~~It is mapped at a depth of ~1.6 km with a clearly visible northeastern flank. A near-horizontal reflector at a depth of ~2.8 km (marked as FR) appears to crosscut the northeastern flank of the curved reflector around CDP ~875. A major reflector down-dipping from the southwestern end of the profile (starting at ~1 km depth) appears to be crosscutting the southwestern flank of the ~~curved~~arcuate reflector (marked as DR1 and DR2). There is also the ~~presence~~impression of~~ several~~ cross-cutting reflectors in the area (red arrows, CF1 and CF2). Higher reflectivity~~ (~1 km)~~ is mapped in the southwestern end of the profile in the depth range of ~1 – 3 km bounded by the reflector DR1. ~~-~~Reflections mapped between CDPs ~~-~~725 – 1200 (SF2, SF3, SF4) and depth ~~up to~~between ~2 – 3 km have an up-dip ~~movement~~direction towards the surface. A dipping

Formatted: Font color: Text 1
Formatted: Font color: Text 1
Formatted: Font color: Text 1
Formatted: Font color: Text 1
Formatted: Font color: Text 1
Formatted: Font color: Text 1
Formatted: Font color: Text 1
Formatted: Font color: Text 1
Formatted: Font color: Text 1
Formatted: Font color: Text 1
Formatted: Font color: Text 1
Formatted: Font color: Text 1
Formatted: Font color: Text 1
Formatted: Font color: Text 1
Formatted: Font color: Text 1

reflectivity is ~~also~~ mapped in the depth range of ~5 – 6 km (marked as LR1 and LR2~~). Compared to the KOSE2018 profile (Fig. 2), the new acquisition and processing produced abundant reflectivity in the area at various depths which was generally absent/poorly focussed, especially around the target area (compare Fig. 5a with Fig. 2~~).

Figure 5b shows the result for 3D KPreSDM~~. The~~ along an inline ~~location is~~position shown by the ~~red~~blue line in Figure 1c. The inline crosscuts the curved CDP line shown in Figure 5a as a straight line~~,~~; therefore the assessment here is only done on a comparative basis. ~~In overall~~Overall, the events for KPreSDM results are much more ~~focused~~focussed and continuous compared to DMO-PoSTM results (compare Fig. 5a with 5b). ~~-~~For example, the continuity of ~~up-dip~~ events ~~between CDPs 725 – 1200 (SF2, SF3,~~ SF1–SF4~~) is~~ are much better imaged. The central ~~curved~~arcuate reflectivity is also delineated better along with other events except for the deeper reflectors ~~imaged at deeper depths~~ marked as LR1 and LR2, for which higher migration velocities are required~~ (compare Fig. . 5a with 5b).~~

Formatted: Font color: Text 1

Formatted: Font color: Text 1

Formatted: Font color: Text 1

Formatted: Font color: Text 1

Formatted: Font color: Text 1

Formatted: Font color: Text 1

Formatted: Font color: Text 1

Formatted: Font color: Text 1

Formatted: Font color: Text 1

Formatted: Font color: Text 1

Formatted: Font color: Text 1

Formatted: Font color: Text 1

Formatted: Font color: Text 1

Formatted: Font color: Text 1

Formatted: Font color: Text 1

Formatted: Font color: Text 1

Formatted: Font color: Text 1

Formatted: Font color: Text 1

Formatted: Font color: Text 1

Formatted: Font color: Text 1

Formatted: Font color: Text 1

Formatted: Font color: Text 1

Formatted: Font color: Text 1

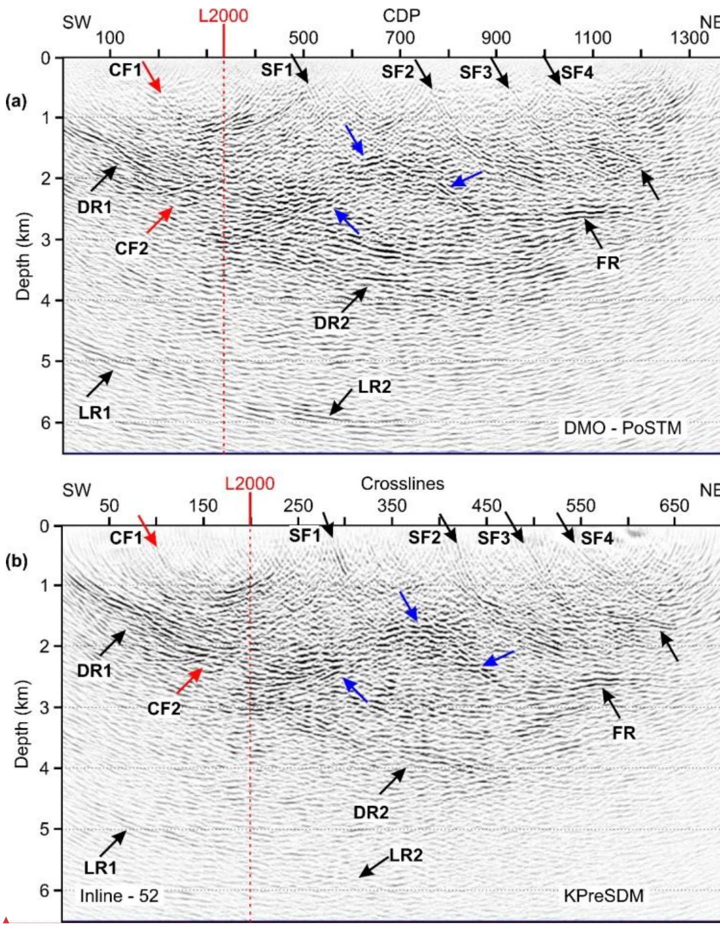

Formatted: Font color: Text 1

Formatted: Font color: Text 1

Figure 5: Imaging results for profile L1000. (a) 2D DMO-PoSTM, (b) 3D KPreSDM (central inline). Black arrows show delineated reflectors at various depths and blue arrows mark the likely extent of the ~~curved~~arcuate reflectivity. Red arrows mark the presence of crosscutting reflectors. The red dashed line shows the intersection location of profile L2000 with L1000.

Formatted: Font color: Text 1

Formatted: Font color: Text 1

Similar to Figure 5, Figure 6 shows imaging results for profile L2000. Figure 6a shows the result for DMO-PoSTM. Black arrows mark different reflectors mapped in the area at various depth levels. ~~Similarly~~Similar to profile L1000, events are less focussed in the first kilometre with some visible reflectivity marked by black arrows (SF1 and SF2~~).~~, not the same events shown in Fig. 5, same is valid for other marked events in Fig. 6). There are hints of several cross-cutting events at the regional scale, although these events are too weak to mark their clear extents (red arrows, CF1 and CF2). The reflector marked as CF1 is delineated clearly up to a depth of ~4 km. Like in profile L1000, a horizontal reflector is ~~also~~ mapped at a depth of ~2.8 km (black arrows, FR). There is also the presence of deeper reflectivity marked by black arrows (LR1, depth ~4 km~~)~~), and LR2 (depth ~5 km). A package of dipping reflectivity at the southeastern end of the profile is also mapped at a depth of ~1 – 2 km (marked as DR). Figure 6b shows results for 3D KPreSDM. The inline location is shown as the ~~red~~blue line in Fig. 1c. Same as for profile L1000, KPreSDM results are better focussed than DMO-PoSTM results (compare Fig. 6a with 6b). A notable difference can be seen for the reflector (CF3, red arrows) ~~at CDP ~450~~ which is almost absent in the DMO-PoSTM result.

Formatted: Font color: Text 1

Formatted: Font color: Text 1

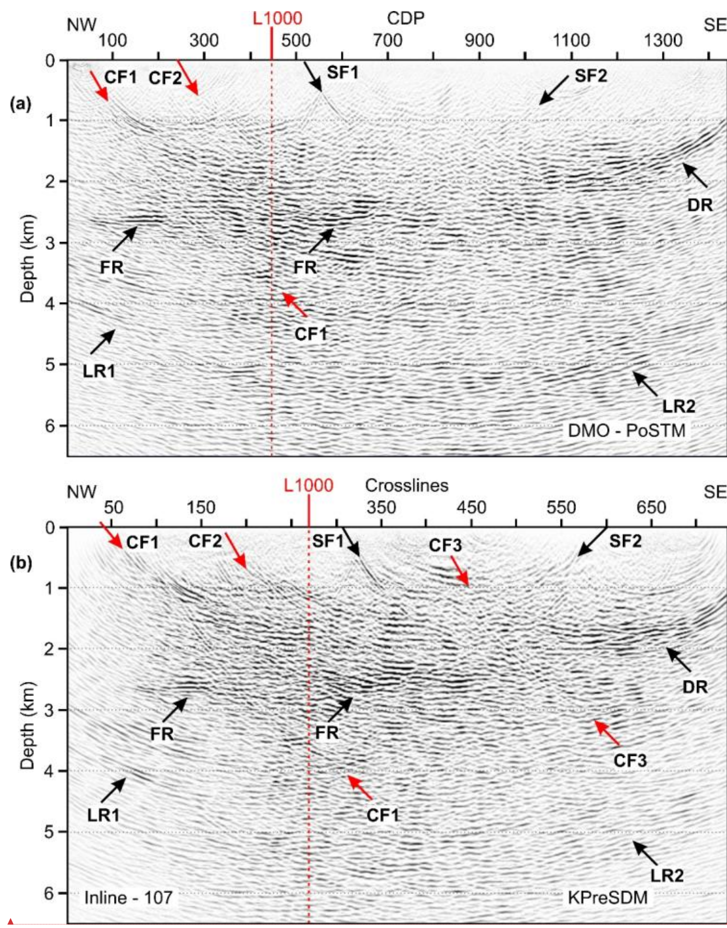

Figure 6: Imaging results for profile L2000. (a) 2D DMO-PoSTM, (b) 3D KPreSDM (central inline). Black arrows show imaged reflectivity at various depths in the area. Red arrows mark the steeply dipping cross-cutting reflectors. The red dashed line shows the intersection location of profile L1000 with L2000.

6. Interpretation and Discussion

~~The interpretation of~~Interpreting the seismic reflectivity ~~mapped~~ in the study area is challenging due to the ~~presence~~availability of only ~~one~~a single drillhole ~~as a direct measurement. However, its origin~~ for calibration. Nevertheless, the observed reflectors

Formatted: Font color: Text 1

Formatted: Font color: Text 1

Formatted: Font color: Text 1

Formatted: Font color: Text 1

Formatted: Font color: Text 1

Formatted: Font color: Text 1

Formatted: Font color: Text 1

can be associated with the ~~presence of~~ mafic–ultramafic intrusions, cross-cutting dykes, ~~faults,~~ fault systems and the lithological contacts~~ present in the area. The top of the magma conduit was~~. The seismic survey successfully imaged ~~with reflections mapped until the~~ the upper part of the interpreted magma conduit down to a depth of ~~~~~approximately 4 – 5 ~~– 6~~ km. ~~The internal structure of~~Internally, the ~~magma~~ conduit ~~seems~~appears more complex than ~~its present understanding~~previously understood, with ~~hints of~~steep fault-like ~~structures~~ features potentially cross-cutting the intrusion. ~~The obtained~~These results were correlated with the ~~initial (i.e. pre-seismic) geological model.~~ pre-seismic geological model to guide interpretation. The two new 2D seismic profiles acquired under the SEEMS DEEP project proved highly beneficial compared to the previously acquired KOSE 2018 profile (compare Fig. 5a with Fig. 2). Seismic imaging produced abundant reflectivity at various depths which is generally absent or otherwise poorly focussed, especially around the target area. This is mainly due to the better optimized/regular acquisition (see Table 1) compared to the previous survey which used only 90 channels with a maximum offset range of ~1800 m, shot-receiver spacing of 20/40 m and use of small explosive charges ~120 – 240 g.

~~For the interpretation,~~ KPreSDM results were preferred ~~as they provided~~ over DMO-PoSTM processing due to improved imaging ~~with better~~ quality and reflector continuity ~~compared to DMO-PoSTM results~~ (see the comparison in ~~Fig~~Figs. 5 and 6). Figure 7 shows the cross-sectional view of the KPreSDM results for both profiles. KPreSDM results are extracted along the same CDP processing line (green line, Fig. 1c) at which the DMO-PoSTM results are shown in Figures 5a and 6a. ~~Figure 7a shows a view towards the west from the east direction.~~ The drill hole is shown along profile L1000. It is to be noted that the processing line intersects the drillhole at a steep angle, so only a part of the drillhole is visible from ~~this~~the shown direction in Figure 7. An enlarged view of the cross-section of the drillhole is shown in the inset on the right. ~~The up-dip reflector is marked by the red arrow in the inset upon projection crosscuts at ~600 m depth section of the drillhole. This reflector possibly represents the cross-cutting diabase encountered during the drilling (see Fig. 1, 3).~~ Depth imaging reveals arcuate and steep reflectors: with the arcuate reflector intersected by the drillhole correlating spatially with the mafic–ultramafic cumulates and coinciding with gravity and magnetic anomalies. This consistency confirms the presence of a deep-seated magma conduit. Although the drillhole does not reach the deepest reflectors; the combined seismic, lithological, and petrophysical evidence supports the existence of vertically extensive mafic–ultramafic packages capable of hosting orthomagmatic critical raw material deposits, most likely including Ni–Cu–PGE sulphides. This interpretation aligns with observations from other intrusions in the Tornio–Näränkävaara Belt, which has been a focus of PGE–Cu–Ni, V–Ti–Fe and Cr exploration, and mining from the 20th century to the present day. In particular, the arcuate reflector near the drillhole likely corresponds to a mafic diabase unit intersected during drilling (see Fig. 3e), with its base coinciding with the onset of mafic–ultramafic cumulates. Deeper reflectivity, particularly in the western parts of the profile indicates several steep reflectors dipping to the east and south (red arrows, Fig. 7b). These likely represent regional-scale faults, including the CF1 fault, which appears to be an overthrust. The CF1 structure coincides spatially with a banded iron formation (BIF) that runs parallel to the magma conduit at depth (marked by red arrow in Fig. 1c). Its association

Formatted: Font color: Text 1
Formatted: Font color: Text 1
Formatted: Font color: Text 1
Formatted: Font color: Text 1
Formatted: Font color: Text 1
Formatted: Font color: Text 1
Formatted: Font color: Text 1
Formatted: Font color: Text 1
Formatted: Font color: Text 1
Formatted: Font color: Text 1
Formatted: Font color: Text 1
Formatted: Font color: Text 1
Formatted: Font color: Text 1
Formatted: Font color: Text 1
Formatted: Font color: Text 1
Formatted: Font color: Text 1

with strong horizontal reflectivity (marked by black arrows) suggests that the BIF may have been structurally overprinted or tectonically emplaced.

The presence of such steep, reflector-defined fault systems further adds structural complexity to the intrusion and its surroundings. These faults may have played a key role in magma emplacement by acting as pathways for ascending melts and mineralising fluids. In addition to orthomagmatic processes, such structures could also have facilitated later-stage hydrothermal activity. The spatial association of the CF1 fault with the BIF suggests potential for hydrothermal overprinting or remobilisation, possibly giving rise to orogenic Au–Co mineralisation. Furthermore, a dense package of southeast-dipping reflectors (marked by blue arrows in Fig. 7b) may represent a continuation or a structurally juxtaposed block of the BIF, previously mapped in the region (Makkonen, 1972). Although this area lacks direct drill control, the structural context supports this interpretation.

Figure 8 compares the KPreSDM seismic results with the pre-existing geological 3D surface model of the Koillismaa conduit, which was developed from the gravity inversion constrained by the drillhole data. The ~~end of the drillhole where mafic-ultramafic rocks were encountered matches~~observed reflectivity aligns well with the ~~top of the arcuate reflectivity. From this, it can be inferred that the curved reflectivity is representative of the mafic intrusion present in the area. Figure 7b again shows KPreSDM results from a view towards the~~modelled conduit geometry, particularly in the central portion of the intrusion. Internally, zones of prominent reflectivity suggest structural or compositional heterogeneity within the mafic–ultramafic body (marked by red arrows). Some of these features may reflect additional lithological contacts or post-emplacement faulting. Black dotted lines show observed reflectors possibly representing faulting, dykes that are present in the area but could not be confirmed due to the lack of direct evidence in terms of borehole or other independent study. The contrasting dip directions of fault zones northeast~~. Higher reflectivity is observed in the western part of the survey with the presence of several steep reflectors dipping towards the east and south direction (see red arrows, compare with CF1 & CF2 in Fig. 5a and CF1 in Fig. 6a, respectively). This possibly shows the presence of multiple larger fault systems present at a regional level in the area. Higher reflectivity only on the~~ and southwest ~~side of the fault 'CF1' suggests it to be an overthrust fault which upon projection coincides with the banded iron formation occurrence that runs parallel to the mafic intrusion (marked by the red arrow in Fig. 1c). A large package of dipping reflectors is mapped on the southeastern end (marked by the blue arrow). There are no direct measurements available in this part of the area, but this higher package of reflectivity could be associated with the Korpua Iron Ore Intrusion (Makkonen, 1972) (see Fig. 1c for location). Interpretation of all the events observed in the seismic image is not~~ of the intrusion could reflect structural uplift, diabase veining, or variations in country rock stratigraphy (see also Figs. 5 & 6). These findings demonstrate the value of integrating seismic and petrophysical datasets in areas with limited drill control. Even in the absence of deep drilling, it is possible ~~at this stage.~~ to identify structural and lithological features critical for mineral systems analysis and for assessing the potential for critical raw materials.

Formatted: Tab stops: Not at 0.89 cm

~~Figure 8 shows a cross-sectional view of KPreSDM results against the initial geological model. The model includes a magma conduit, which was built based on the density model obtained from gravity inversion with constraints from the drillhole data. Figure 8a shows the view towards the west direction (same as in Fig. 7a). The modelled mafic intrusion correlates well with the mapped reflectivity. It is well-bounded within the mapped reflectivity in the central area as well as some prominent internal reflectivity (red arrows) which means that the internal geological structure of the mafic intrusion bears more complexity than what was thought of as a single lithological unit. Figure 8b is the same as Figure 8a with the projected outline of the magma conduit (dashed contour). Black dotted lines show different mapped reflectors in the area. There are impressions of major faults/lithological units cross-cutting the intrusion otherwise too weak to be marked distinctively. It can be inferred that there might be a second magma conduit between the exposed Koillismaa intrusion and Näränkävaara intrusion of the KLIC. The up-dip direction of the mapped faults above the magma conduit reached by the drilling faces opposite directions towards the northeast and southwest directions. These may be attributed to different lithological units resulting from the uplifting of the known magma conduit, or, they represent diabase veins mapped on the surface area.~~

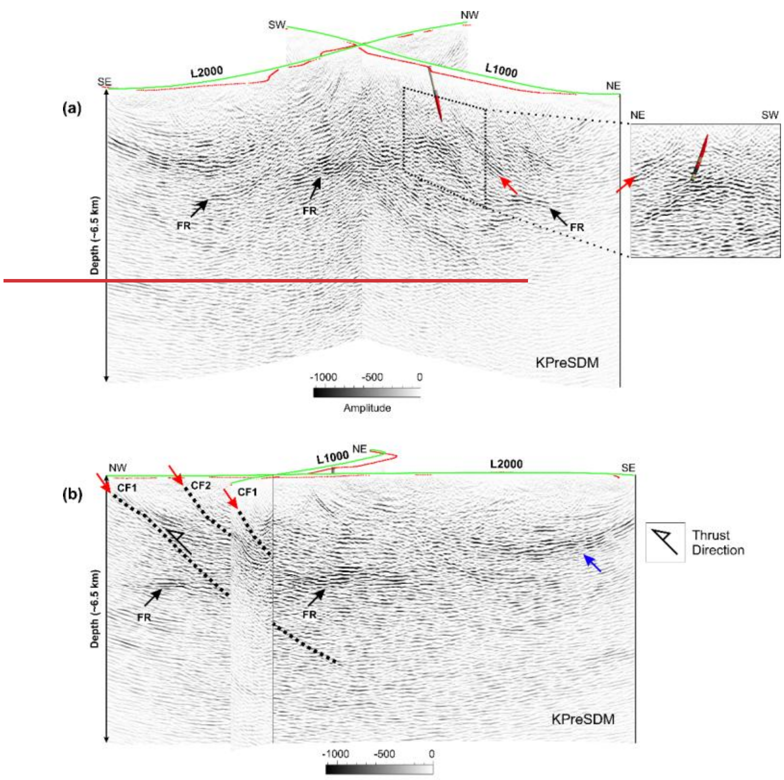

SW
NW
L2000
L1000
SE
NE
(a)
NE
SW
FR
FR
FR
Depth (~6.5 km)
KPreSDM
-1000
-500
0
Amplitude
NW
L1000
NE
L2000
SE
(b)
CF1
CF2
CF1
Thrust
Direction
FR
FR
Depth (~6.5 km)
KPreSDM
-1000
-500
0
Amplitude

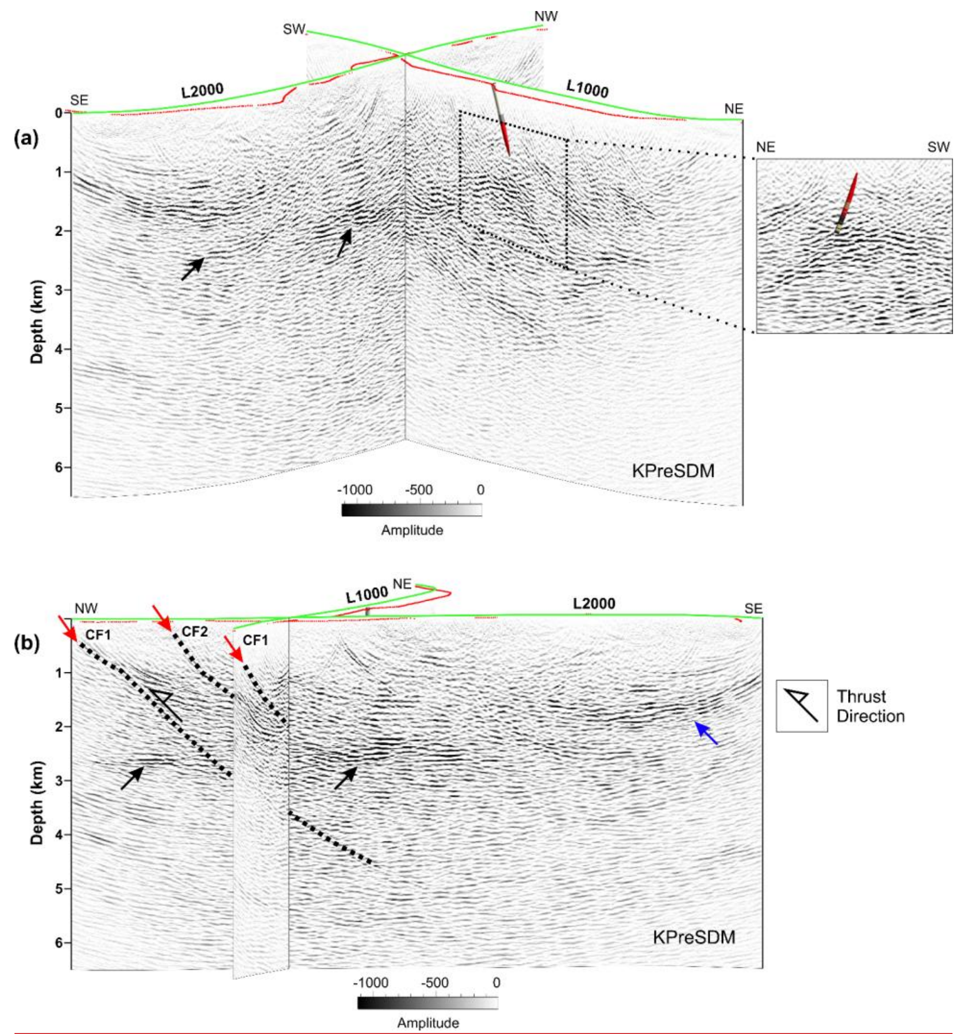

Figure 7: Cross-sectional view of (a) KPreSDM result, (b) same as (a) from a different view angle perspective. ~~Insets~~Inset in (a) show an enlarged section ~~of (a)~~ around the ~~borehole~~drillhole location. Red, blue, and black arrows highlight reflectors used for the interpretation. The green line is the CDP line shown in Figure 1c and the red dots show the source locations along the profiles. Dotted black lines represent mapped faults in the area.

Formatted: Font color: Text 1

Formatted: Font color: Text 1

Formatted: Font color: Text 1

Formatted: Font color: Text 1

Formatted: Font color: Text 1

Formatted: Font color: Text 1

Formatted: Font color: Text 1

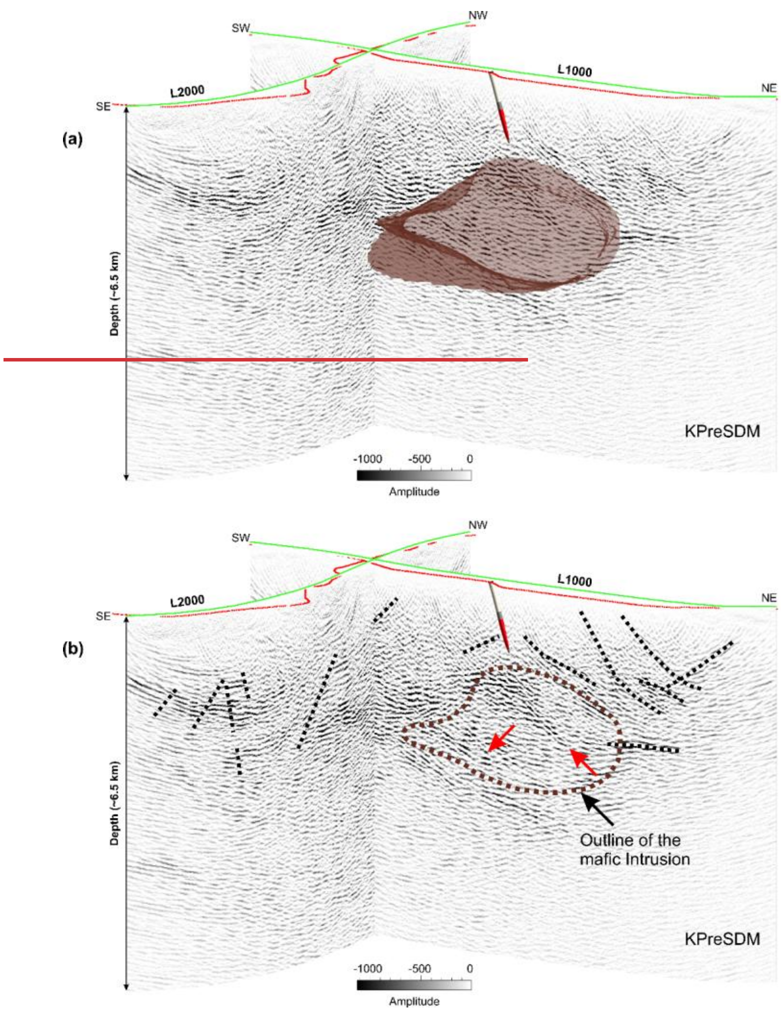
SW
NW
L1000
L2000
SE
NE
(a)
Depth (~6.5 km)
KPreSDM
-1000 -500 0
Amplitude
SW
NW
L1000
L2000
SE
NE
(b)
Depth (~6.5 km)
Outline of the
mafic Intrusion
KPreSDM
-1000 -500 0
Amplitude

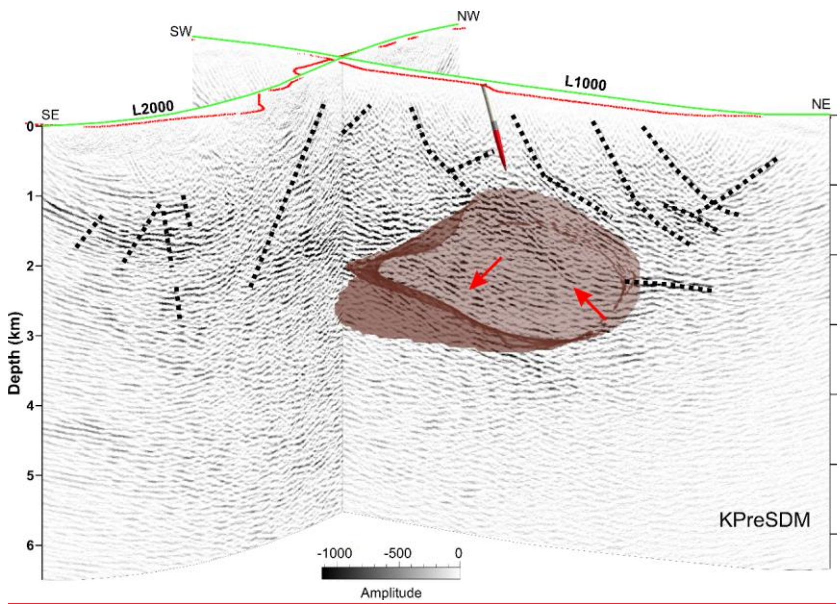

Figure 8: ~~(a)~~ Cross-sectional view of KPreSDM with the initial geological model of the mafic intrusion ~~(dashed contour) (b) same as (a) with the highlighted outline of~~and the drillhole. The red arrow marks the ~~intrusion (dashed closed contour).~~delineated internal reflectivity within the magma conduit. Black dashed lines ~~show the main events.~~shows the possible faults, dykes or lithological contacts present in the area. The green line shows the CDP line shown in Figure ~~3c~~1c, and the red dots show the source location along the profiles.

7. Conclusions

Two regional seismic profiles were acquired within the SEEMS DEEP project to map the regional reflectivity and to constrain the geometrical architecture of the deep-seated Koillismaa magma conduit. Depth-domain imaging (KPreSDM) provided ~~more focused~~focussed images with better continuity than DMO-PoSTM imaging. Several reflections are mapped at various depths whose origin can be associated with the presence of dykes, faults~~,~~ and lithological contacts in the area. Regional faults were ~~also~~ imaged with reflectivity down to a depth of ~4 – 5 ~~– 6~~ km. The ~~top of the~~ magma conduit associated with KLIC ~~is~~has been successfully revealed which was one of the main aims of the SEEMS DEEP project. The mapped internal structure of the magma conduit seems more complex than its present understanding with ~~hints of fault-like structures cross-cutting the~~ prominent internal reflectivity suggesting a more structural or compositional heterogeneity within the mafic-ultramafic body. The extensive mafic-ultramafic intrusion~~. It is interpreted that there~~ has the potential to host critical raw material deposits of Ni-Cu-PGE sulphide type. Overthrusting has been observed in the western part of the study area with several steep regional-

Formatted: Font color: Text 1
Formatted: Font color: Text 1
Formatted: Font color: Text 1
Formatted: Font color: Text 1
Formatted: Font color: Text 1
Formatted: Font color: Text 1
Formatted: Font color: Text 1
Formatted: Font color: Text 1
Formatted: Font color: Text 1
Formatted: Font color: Text 1
Formatted: Font color: Text 1
Formatted: Font color: Text 1
Formatted: Font color: Text 1
Formatted: Font color: Text 1
Formatted: Font color: Text 1
Formatted: Font color: Text 1
Formatted: Font color: Text 1
Formatted: Font color: Text 1

scale fault systems which was not known prior to the seismic study. These steep faults might ~~be a second~~have played an important role in magma ~~conduit between the exposed Koillismaa intrusion~~emplacement acting as pathways for ascending melts and ~~Näränkävaara intrusion of the KLIC~~mineralisation fluids. The two profiles' cross-cutting proximity proved advantageous in constraining the mapped regional-scale reflectivity in the area, leading to a more detailed understanding of the structural geology associated with the mafic intrusion. This will ~~tremendously~~ help ~~build~~in building a more detailed geological model of the Koillismaa area.

Formatted: Font color: Text 1

Formatted: Font color: Text 1

Formatted: Font color: Text 1

Data availability

Data associated with this research are available per request to the project coordinator: Uula Autio (uula.autio@gtk.fi), Geological Survey of Finland, Vuorimiehentie 5, 02151 Espoo, Finland.

Team list

Formatted: Font color: Text 1

Jochen Kamm, Cedric Patzer, Veera Pajunen, Toni Eerola, Tuija Luhta, Viveka Laakso, Olli Salmela (Geological Survey of Finland (GTK), Finland); Mathieu Darnet, Francois Bretaudeau, Simon Vedrine, Bitnarae Kim, Florent Beaubois, Jacques Deparis (French Geological Survey (BRGM), France); Szymon Oryński (Institute of Geophysics, Polish Academy of Sciences Warsaw (IGF PAN), Poland); Thomas Kalscheuer, Karol Sierszen, Mehrdad Bastani (Uppsala University, Sweden); Catherine Truffert, Fabrice Vermeersch, Julien Gance (IRIS Instruments, France); Łukasz Sito (Geopartner Geofizyka, Poland); Antti Kivinen, Janne Kaukolinna (GRM-services Oy, Finland); Yuriy Koltun (Laakso Minerals Oy, Finland)

Formatted: Font color: Text 1

Formatted: Font color: Text 1

Author contribution

AG, MM, and SH obtained funding. BS, AG, and MM designed the 2D survey. BS, AG, MM, SH, and MW contributed to the data acquisition. BS performed the signal processing for the seismic dataset used for DMO-PoSTM and PreSDM. AG contributed to the implementation of curvelet denoising to the seismic dataset. BS and MM QC'ed the signal processing results at various stages. BS, AG, and MM interpreted the results. BS, MM, and TK contributed to the interpretation of the results. BS wrote the manuscript's main content with major contributions from AG & MM, and other authors. All authors contributed to the final interpretation and discussion of the results.

Competing interests

Formatted: Font color: Text 1

The contact author has declared that neither they nor their co-authors have competing interests. However, one of the authors (MM) is a member of the editorial board of Solid Earth.

Acknowledgments

We are greatly thankful to the entire SEEMS DEEP field crew for helping in the acquisition of the data. 3C seismic receivers were used from the FINNSIP seismic instrument pool (FLEX-EPOS, Research Council of Finland 328776) and electric field sensors from the Geophysical Instrument Pool Potsdam (GIPP) were used. Globe Claritas™ under the academic license from Petrosys Ltd. and Seismic Unix ~~was~~were used for the data processing and visualization. Thanks to Mira Geoscience for special licensing terms to use the Geoscience Analyst software. We thank TU Freiberg, Germany for allowing us to use their in-house code for depth-domain imaging. ~~Curvelet~~The curvelet denoising algorithm was taken from the CURVELAB project (www.curvelet.org). We acknowledge Google for using the map of Finland (Map data ©2025 Google, GeoBasis-DE/BKG (©2009)).

Financial support

SEEMS DEEP is a part of the ERA-MIN3 Joint call 2021 (National funding agencies: Finland: Business Finland (640/31/2022), France: ANR (ANR-22-MIN3-0006-02), Sweden: VINNOVA (2022-00209), Poland: NCBR (ERA-MIN3/1/113/SEEMSDEEP/2022).

Formatted: Space Before: Auto, After: Auto

Formatted: English (India)

References

Formatted: Font color: Text 1

~~Alapieti, T.: The Koillismaa Layered Igneous Complex, Finland - Its Structure, Mineralogy and Geochemistry with Emphasis on the Distribution of Chromium, The Koillismaa Layered Igneous Complex, Finland - Its Structure, Mineralogy and Geochemistry with Emphasis on the Distribution of Chromium, 1982.~~

~~EU Critical Raw Materials Act: Regulation (EU) 2024/1252 of the European Parliament and of the Council of 11 April 2024 establishing a framework for ensuring a secure and sustainable supply of critical raw materials and amending Regulations (EU) No 168/2013, (EU) 2018/858, (EU) 2018/1724 and (EU) 2019/1020.: https://eur-lex.europa.eu/eli/reg/2024/1252/oj, last access: 12 November 2024.~~

~~Autio, U., Darnet, M., Górszczyk, A., Kamm, J., Heinonen, S., Malinowski, M., Kim, B., Singh, B., Vedrine, S., Bretaudeau, F., Patzer, C., Karinen, T., Kalscheuer, T., Truffert, C., Wojdyła, M., Kivinen, A., and Koltun, Y.: Integrating Seismic and Electromagnetic Methods for Deep Mineral Exploration – Results from the SEEMS DEEP Project, NSG 2024 5th Conference on Geophysics for Mineral Exploration and Mining, 1–5, https://doi.org/10.3997/2214-4609.202420147, 2024.~~

~~Barnes, S. J., Cruden, A. R., Arndt, N., and Saumur, B. M.: The mineral system approach applied to magmatic Ni–Cu–PGE sulphide deposits, Ore Geology Reviews, 76, 296–316, https://doi.org/10.1016/j.oregeorev.2015.06.012, 2016.~~

~~Bellefleur, G., Schetselaar, E., White, D., Miah, K., and Dueck, P.: 3D seismic imaging of the Lalor volcanogenic massive sulphide deposit, Manitoba, Canada, Geophysical Prospecting, 63, 813–832, https://doi.org/10.1111/1365-2478.12236, 2015.~~

~~Bleeker, W. and Ernst, R.: Short-lived mantle generated magmatic events and their dyke swarms: The key unlocking Earth's paleogeographic record back to 2.6 Ga, Dyke Swarms – Time Markers of Crustal Evolution, 3–26, 2006.~~

~~Cheraghi, S., Naghizadeh, M., Snyder, D., Haugaard, R., and Gemmell, T.: High-resolution seismic imaging of crooked two-dimensional profiles in greenstone belts of the Canadian shield: results from the Swayze area, Ontario, Canada, Geophysical Prospecting, 68, 62–81, https://doi.org/10.1111/1365-2478.12854, 2020.~~

~~Ciborowski, T. J. R., Kerr, A. C., Ernst, R. E., McDonald, I., Minifie, M. J., Harlan, S. S., and Millar, I. L.: The Early Proterozoic Matachewan Large Igneous Province: Geochemistry, Petrogenesis, and Implications for Earth Evolution, Journal of Petrology, 56, 1459–1494, https://doi.org/10.1093/petrology/egv038, 2015.~~

~~European Commission Report: Directorate-General for Internal Market, Industry, Entrepreneurship and SMEs (European Commission), Grohol, M., and Veeh, C.: Study on the critical raw materials for the EU 2023: final report, Publications Office of the European Union, 2023.~~

~~Gislason, G., Heinonen, S., Salmirinne, H., Konnunaho, J., and Karinen, T.: KOSE-Koillismaa Seismic Exploration survey: Acquisition, processing and interpretation, GTK: n työraportti-GTK Open File Work Report, 2019.~~

~~Górszczyk, A., Malinowski, M., and Bellefleur, G.: Enhancing 3D post-stack seismic data acquired in hardrock environment using 2D curvelet transform, Geophysical Prospecting, 63, 903–918, https://doi.org/10.1111/1365-2478.12234, 2015.~~

~~Heaman, L. M.: Global mafic magmatism at 2.45 Ga: Remnants of an ancient large igneous province?, Geology, 25, 299–302, https://doi.org/10.1130/0091-7613(1997)025<0299:GMMAGR>2.3.CO;2, 1997.~~

~~Heinonen, S., Nousiainen, M., Karinen, T., and Häkkinen, T.: Are Seismic P-Wave Velocities Capable of Revealing The Deep-Seated Prospective Intrusion?, NSG2022 4th Conference on Geophysics for Mineral Exploration and Mining, 1–5, https://doi.org/10.3997/2214-4609.202220167, 2022.~~

~~Hloušek, F., Hellwig, O., and Buske, S.: Improved structural characterization of the Earth's crust at the German Continental Deep Drilling Site using advanced seismic imaging techniques, Journal of Geophysical Research: Solid Earth, 120, 6943–6959, https://doi.org/10.1002/2015JB012330, 2015.~~

~~Karinen, T.: The Koillismaa intrusion, northeastern Finland: evidence for PGE reef forming processes in the layered series, Geological Survey of Finland, 2010.~~

~~Karinen, T., Heinonen, S., Konnunaho, J., Salmirinne, H., Lahti, I., and Salo, A.: Koillismaa Deep Hole–Solving the mystery of a geophysical anomaly, in: Lithosphere 2021, eleventh symposium on structure, composition and evolution of the lithosphere, Programme and Extended Abstracts, 55–58, 2021a.~~

~~Karinen, T., Salmirinne, H., Lahti, I., Konnunaho, J., S., H., and Salo, A.: The Koillismaa Deep Hole: insight to anomalous mafic intrusion, 38–41, https://doi.org/10.31241/ARLIN.2021.009, 2021b.~~

~~Köykkä, J., Lahtinen, R., and Manninen, T.: Tectonic evolution, volcanic features and geochemistry of the Paleoproterozoic Salla belt, northern Fennoscandia: From 2.52 to 2.40 Ga LIP stages to ca. 1.92–1.90 Ga collision, Precambrian Research, 371, 106597, https://doi.org/10.1016/j.precamres.2022.106597, 2022.~~

~~Makkonen, V.: Korpuan Jatkotutkimus. Rautaruukki Oy Research Report Ou 16/72, 1972.~~

~~Malehmir, A., Durrheim, R., Bellefleur, G., Urosevic, M., Juhlin, C., White, D. J., Milkereit, B., and Campbell, G.: Seismic methods in mineral exploration and mine planning: A general overview of past and present case histories and a look into the future, GEOPHYSICS, 77, WC173–WC190, https://doi.org/10.1190/geo2012-0028.1, 2012.~~

~~Malehmir, A., Maries, G., Bäckström, E., Schön, M., and Marsden, P.: Developing cost-effective seismic mineral exploration methods using a landstreamer and a drophammer, Sci Rep, 7, 10325, https://doi.org/10.1038/s41598-017-10451-6, 2017.~~

~~Malinowski, M., Brodic, B., Martinkauppi, I., Koskela, E., and Laakso, V.: Distributed acoustic sensing vertical seismic profiling in hardrock environment: case study from Koillismaa drillhole, Finland, 84th EAGE Annual Conference & Exhibition, 1–5, https://doi.org/10.3997/2214-4609.2023101043, 2023.~~

~~Malinowski, M., Heinonen, S., Górszczyk, A., Singh, B., Sito, L., Karinen, T., and Autio, U.: A Novel 3D Seismic Survey over the 2.5-2.4 Ga Koillismaa Layered Intrusion Complex, Finland, NSG 2024 5th Conference on Geophysics for Mineral Exploration and Mining, 1–5, https://doi.org/10.3997/2214-4609.202420077, 2024.~~

~~Markovic, M., Maries, G., Malehmir, A., Ketelhodt, J. von, Bäckström, E., Schön, M., and Marsden, P.: Deep reflection seismic imaging of iron-oxide deposits in the Ludvika mining area of central Sweden, Geophysical Prospecting, 68, 7–23, https://doi.org/10.1111/1365-2478.12855, 2020.~~

~~Milkereit, B., Berrer, E. K., King, A. R., Watts, A. H., Roberts, B., Erick, A., Eaton, D. W., Wu, J., and Salisbury, M. H.: Development of 3-D seismic exploration technology for deep nickel-copper deposits—A case history from the Sudbury basin, Canada3-D Seismic Exploration Technology, Geophysics, 65, 1890–1899, https://doi.org/10.1190/1.1444873, 2000.~~

~~Nedimović, M. R. and West, G. F.: Crooked-line 2D seismic reflection imaging in crystalline terrains: Part 2, migration, GEOPHYSICS, 68, 286–296, https://doi.org/10.1190/1.1543214, 2003.~~

~~Nousiainen, M., Heinonen, S., and Karinen, T.: Petrophysics of the Koillismaa drill hole, in: TWELFTH SYMPOSIUM ON THE STRUCTURE, COMPOSITION AND EVOLUTION OF THE LITHOSPHERE, 131, 2022.~~

~~Ripley, E. M. and Li, C.: Chapter 3 - Metallic Ore Deposits Associated With Mafic to Ultramafic Igneous Rocks, in: Processes and Ore Deposits of Ultramafic-Mafic Magmas through Space and Time, edited by: Mondal, S. K. and Griffin, W. L., Elsevier, 79–111, https://doi.org/10.1016/B978-0-12-811159-8.00004-4, 2018.~~

~~Salmirinne, H. and Iljina, M.: Koillismaan kerrosintruusiokompleksin tulokanavamuodostuman painovoimatulkinta ja alueen malmimahdollisuudet (osa 1), Geologian Tutkimuskeskus Q, 21, 1, 2003.~~

~~Schulz, K. J., Woodruff, L. G., Nicholson, S. W., Ii, R. R. S., Piatak, N. M., Chandler, V. W., and Mars, J. L.: Occurrence model for magmatic sulfide-rich nickel-copper-(platinum-group element) deposits related to mafic and ultramafic dike-sill complexes, Scientific Investigations Report, U.S. Geological Survey, https://doi.org/10.3133/sir20105070I, 2014.~~

~~Singh, B. and Malinowski, M.: Depth Imaging of Crooked Seismic Profiles in Hardrock Environment: Is 2D Enough?, NSG2022 4th Conference on Geophysics for Mineral Exploration and Mining, 1–5, https://doi.org/10.3997/2214-4609.202220169, 2022.~~

~~Singh, B. and Malinowski, M.: Seismic Imaging of Mineral Exploration Targets: Evaluation of Ray-vs. Wave-Equation-Based Pre-Stack Depth Migrations for Crooked 2D Profiles, Minerals, 13, 264, 2023.~~

~~Singh, B., Górszczyk, A., Malinowski, M., Heinonen, S., Autio, U., Wojdyła, M., and Kamm, J.: Mapping Regional Reflectivity of Mineral-prone Koillismaa Layered Intrusion Complex in Northern Finland using Crooked Seismic Profiles, NSG 2024 5th Conference on Geophysics for Mineral Exploration and Mining, 1–5, https://doi.org/10.3997/2214-4609.202420162, 2024.~~

~~Skyttä, P., Piippo, S., Kloppenburg, A., and Corti, G.: 2. 45 Ga break-up of the Archaean continent in Northern Fennoscandia: Rifting dynamics and the role of inherited structures within the Archaean basement, Precambrian Research, 324, 303–323, https://doi.org/10.1016/j.precamres.2019.02.004, 2019.~~

~~Tirronniemi, J., Bischoff, A., Malinowski, M., Autio, U., Karinen, T., Lukkarinen, V., Heinonen, S., Mikkola, P., Leskelä, T., and Patzer, C.: Koillismaa Deep Hole–Final Report, GTK Open File Work Report, 73 pp, 2024.~~

Alapieti, T.: The Koillismaa Layered Igneous Complex, Finland - Its Structure, Mineralogy and Geochemistry with Emphasis on the Distribution of Chromium, Geological Survey of Finland, Bulletin, 319, 116 pp., https://hakku.gtk.fi/en/publications?id=506, 1982.

Alapieti, T. and Lahtinen, J.: Platinum-group element mineralization in layered intrusions of northern Finland and the Kola Peninsula, Russia, The geology, geochemistry, mineralogy and mineral beneficiation of platinum-group elements. Canadian Institute of Mining, Metallurgy and Petroleum, CIM Special Volume, 54, 507–546, 2002.

EU Critical Raw Materials Act: Regulation (EU) 2024/1252 of the European Parliament and of the Council of 11 April 2024 establishing a framework for ensuring a secure and sustainable supply of critical raw materials and amending Regulations (EU) No 168/2013, (EU) 2018/858, (EU) 2018/1724 and (EU) 2019/1020.: https://eur-lex.europa.eu/eli/reg/2024/1252/oj, last access: 12 November 2024.

Autio, U., Darnet, M., Górszczyk, A., Kamm, J., Heinonen, S., Malinowski, M., Kim, B., Singh, B., Vedrine, S., Bretaudeau, F., Patzer, C., Karinen, T., Kalscheuer, T., Truffert, C., Wojdyła, M., Kivinen, A., and Koltun, Y.: Integrating Seismic and Electromagnetic Methods for Deep Mineral Exploration – Results from the SEEMS DEEP Project, NSG 2024 5th Conference on Geophysics for Mineral Exploration and Mining, 1–5, https://doi.org/10.3997/2214-4609.202420147, 2024.

Barnes, S. J., Cruden, A. R., Arndt, N., and Saumur, B. M.: The mineral system approach applied to magmatic Ni–Cu–PGE sulphide deposits, Ore Geology Reviews, 76, 296–316, https://doi.org/10.1016/j.oregeorev.2015.06.012, 2016.

Bedrock of Finland – DigiKP Digital Map Database, Version 2.3; Geological Survey of Finland: Espoo, Finland, 2019. Available online: https://gtkdata.gtk.fi/Kalliopera/index.html (accessed on 19 June 2025).

Bellefleur, G., Schetselaar, E., White, D., Miah, K., and Dueck, P.: 3D seismic imaging of the Lalor volcanogenic massive sulphide deposit, Manitoba, Canada, Geophysical Prospecting, 63, 813–832, https://doi.org/10.1111/1365-2478.12236, 2015.

Bleeker, W. and Ernst, R.: Short-lived mantle generated magmatic events and their dyke swarms: The key unlocking Earth's paleogeographic record back to 2.6 Ga, 5th International Dyke Conference: Dyke Swarms - Time Markers of Crustal Evolution, IDC-5, 3–26, 2006.

Cheraghi, S., Naghizadeh, M., Snyder, D., Haugaard, R., and Gemmell, T.: High-resolution seismic imaging of crooked two-dimensional profiles in greenstone belts of the Canadian shield: results from the Swayze area, Ontario, Canada, Geophysical Prospecting, 68, 62–81, https://doi.org/10.1111/1365-2478.12854, 2020.

Ciborowski, T. J. R., Kerr, A. C., Ernst, R. E., McDonald, I., Minifie, M. J., Harlan, S. S., and Millar, I. L.: The Early Proterozoic Matachewan Large Igneous Province: Geochemistry, Petrogenesis, and Implications for Earth Evolution, Journal of Petrology, 56, 1459–1494, https://doi.org/10.1093/petrology/egv038, 2015.

European Commission: Directorate-General for Internal Market, Industry, Entrepreneurship and SMEs, Grohol, M., and Veeh, C.: Study on the critical raw materials for the EU 2023 - final report, Publications Office of the European Union, https://data.europa.eu/doi/10.2873/725585, 2023.

Gislason, G., Heinonen, S., Salmirinne, H., Konnunaho, J., and Karinen, T.: KOSE-Koillismaa Seismic Exploration survey: Acquisition, processing and interpretation, GTK: n työraportti-GTK Open File Work Report, 101/2018, 33 pp., https://hakku.gtk.fi/en/publications?id=21695, 2019.

Górszczyk, A., Malinowski, M., and Bellefleur, G.: Enhancing 3D post-stack seismic data acquired in hardrock environment using 2D curvelet transform, Geophysical Prospecting, 63, 903–918, https://doi.org/10.1111/1365-2478.12234, 2015.

Heaman, L. M.: Global mafic magmatism at 2.45 Ga: Remnants of an ancient large igneous province?, Geology, 25, 299–302, https://doi.org/10.1130/0091-7613(1997)025<0299:GMMAGR>2.3.CO;2, 1997.

Heinonen, S., Nousiainen, M., Karinen, T., and Häkkinen, T.: Are Seismic P-Wave Velocities Capable of Revealing The Deep-Seated Prospective Intrusion?, NSG2022 4th Conference on Geophysics for Mineral Exploration and Mining, 1–5, https://doi.org/10.3997/2214-4609.202220167, 2022.

Hloušek, F., Hellwig, O., and Buske, S.: Improved structural characterization of the Earth's crust at the German Continental Deep Drilling Site using advanced seismic imaging techniques, Journal of Geophysical Research: Solid Earth, 120, 6943–6959, https://doi.org/10.1002/2015JB012330, 2015.

Järvinen, V., Halkoaho, T., Konnunaho, J., Heinonen, J. S., and Rämö, O. T.: Parental magma, magmatic stratigraphy, and reef-type PGE enrichment of the 2.44-Ga mafic-ultramafic Näränkävaara layered intrusion, Northern Finland, Mineralium Deposita, 55, 1535–1560, https://doi.org/10.1007/s00126-019-00934-z, 2020.

Järvinen, V., Karampelas, N., Rämö, T., Halkoaho, T., Törmänen, T., Mikkola, P., and Lahaye, Y.: Secular change of tectonic setting in the Archean Takanen greenstone belt, northeastern Karelia Province, Fennoscandian Shield, Bulletin of the Geological Society of Finland, 95, 107–134, https://doi.org/10.17741/bgsf/95.2.002, 2023.

Karinen, T.: The Koillismaa intrusion, northeastern Finland: evidence for PGE reef forming processes in the layered series, Geological Survey of Finland, https://hakku.gtk.fi/en/publications?id=22154, 2010.

Karinen, T., Heinonen, S., Konnunaho, J., Salmirinne, H., Lahti, I., and Salo, A.: Koillismaa Deep Hole–Solving the mystery of a geophysical anomaly, in: Lithosphere 2021, eleventh symposium on structure, composition and evolution of the lithosphere, Programme and Extended Abstracts, 55–58, https://research.fi/en/results/publication/0374173621, 2021a.

Karinen, T., Kurhila, M., Moilanen, M., Konnunaho, J., Salmirinne, H., and Tirroniemi, J.: Supercooling and marginal reversal formation in the Koillismaa Deep Intrusion: Implications for parental magma composition in the 2.44 Ga Tornio–Näränkävaara Belt. Contributions to Mineralogy and Petrology, 2025. (Accepted)

Karinen, T., Salmirinne, H., Lahti, I., Konnunaho, J., S., H., and Salo, A.: The Koillismaa Deep Hole: insight to anomalous mafic intrusion, 38–41, https://doi.org/10.31241/ARLIN.2021.009, 2021b.

Kärki, A. and Laajoki, K.: An interlinked system of folds and ductile shear zones—late stage Svecokarelian deformation in the central Fennoscandian Shield, Finland, Journal of Structural Geology, 17, 1233–1247, https://doi.org/10.1016/0191-8141(95)00006-Y, 1995.

Köykkä, J., Lahtinen, R., and Manninen, T.: Tectonic evolution, volcanic features and geochemistry of the Paleoproterozoic Salla belt, northern Fennoscandia: From 2.52 to 2.40 Ga LIP stages to ca. 1.92–1.90 Ga collision, Precambrian Research, 371, 106597, https://doi.org/10.1016/j.precamres.2022.106597, 2022.

Makkonen, V.: Korpuan Jatkotutkimus. Rautaruukki Oy Research Report Ou 16/72, 1972.

Malehmir, A., Durrheim, R., Bellefleur, G., Urosevic, M., Juhlin, C., White, D. J., Milkereit, B., and Campbell, G.: Seismic methods in mineral exploration and mine planning: A general overview of past and present case histories and a look into the future, Geophysics, 77, WC173–WC190, https://doi.org/10.1190/geo2012-0028.1, 2012.

Malehmir, A., Maries, G., Bäckström, E., Schön, M., and Marsden, P.: Developing cost-effective seismic mineral exploration methods using a landstreamer and a drophammer, Scientific Reports, 7, 10325, https://doi.org/10.1038/s41598-017-10451-6, 2017.

Malinowski, M., Brodic, B., Martinkauppi, I., Koskela, E., and Laakso, V.: Distributed acoustic sensing vertical seismic profiling in hardrock environment: case study from Koillismaa drillhole, Finland, 84th EAGE Annual Conference & Exhibition, 1–5, https://doi.org/10.3997/2214-4609.2023101043, 2023.

Malinowski, M., Heinonen, S., Górszczyk, A., Singh, B., Sito, L., Karinen, T., and Autio, U.: A Novel 3D Seismic Survey over the 2.5-2.4 Ga Koillismaa Layered Intrusion Complex, Finland, NSG 2024 5th Conference on Geophysics for Mineral Exploration and Mining, 1–5, https://doi.org/10.3997/2214-4609.202420077, 2024.

Markovic, M., Maries, G., Malehmir, A., Ketelhodt, J. von, Bäckström, E., Schön, M., and Marsden, P.: Deep reflection seismic imaging of iron-oxide deposits in the Ludvika mining area of central Sweden, Geophysical Prospecting, 68, 7–23, https://doi.org/10.1111/1365-2478.12855, 2020.

Milkereit, B., Berrer, E. K., King, A. R., Watts, A. H., Roberts, B., Erick, A., Eaton, D. W., Wu, J., and Salisbury, M. H.: Development of 3-D seismic exploration technology for deep nickel-copper deposits—A case history from the Sudbury basin, Canada3-D Seismic Exploration Technology, Geophysics, 65, 1890–1899, https://doi.org/10.1190/1.1444873, 2000.

Nedimović, M. R. and West, G. F.: Crooked-line 2D seismic reflection imaging in crystalline terrains: Part 2, migration, Geophysics, 68, 286–296, https://doi.org/10.1190/1.1543214, 2003.

Nousiainen, M., Heinonen, S., and Karinen, T.: Petrophysics of the Koillismaa drill hole, in: Lithosphere 2022: twelfth symposium on the structure, composition and evolution of the lithosphere, 131-134, http://hdl.handle.net/10138/350596, 2022.

Ripley, E. M. and Li, C.: Chapter 3 - Metallic Ore Deposits Associated With Mafic to Ultramafic Igneous Rocks, in: Processes and Ore Deposits of Ultramafic-Mafic Magmas through Space and Time, edited by: Mondal, S. K. and Griffin, W. L., Elsevier, 79–111, https://doi.org/10.1016/B978-0-12-811159-8.00004-4, 2018.

Salmirinne, H. and Iljina, M.: Koillismaan kerrosintruusiokompleksin tulokanavamuodostuman painovoimatulkinta ja alueen malmimahdollisuudet (osa 1), GTK: n arkistoraportit, https://hakku.gtk.fi/en/publications?id=14126, 2003.

Schulz, K. J., Woodruff, L. G., Nicholson, S. W., Ii, R. R. S., Piatak, N. M., Chandler, V. W., and Mars, J. L.: Occurrence model for magmatic sulfide-rich nickel-copper-(platinum-group element) deposits related to mafic and ultramafic dike-sill complexes, Scientific Investigations Report, U.S. Geological Survey, https://doi.org/10.3133/sir20105070I, 2014.

Singh, B. and Malinowski, M.: Depth Imaging of Crooked Seismic Profiles in Hardrock Environment: Is 2D Enough?, NSG2022 4th Conference on Geophysics for Mineral Exploration and Mining, 1–5, https://doi.org/10.3997/2214-4609.202220169, 2022.

Singh, B. and Malinowski, M.: Seismic Imaging of Mineral Exploration Targets: Evaluation of Ray- vs. Wave-Equation-Based Pre-Stack Depth Migrations for Crooked 2D Profiles, Minerals, 13, 264, https://doi.org/10.3390/min13020264, 2023.

Skyttä, P., Piippo, S., Kloppenburg, A., and Corti, G.: 2. 45 Ga break-up of the Archaean continent in Northern Fennoscandia: Rifting dynamics and the role of inherited structures within the Archaean basement, Precambrian Research, 324, 303–323, https://doi.org/10.1016/j.precamres.2019.02.004, 2019.

Tirronniemi, J., Bischoff, A., Malinowski, M., Autio, U., Karinen, T., Lukkarinen, V., Heinonen, S., Mikkola, P., Leskelä, T., Patzer, C., Pipponen, K., Nousiainen, M., Hakala, P., Martinkauppi, I., Anttilainen, T., Engström, J., Konnunaho, J., Telkkälä,

Formatted: Line spacing: single

P., and Haavikko, S.: Koillismaa Deep Hole Final Report, GTK Open File Work Report, 77 pp, https://hakku.gtk.fi/en/publications?id=22284, 2024.

Formatted: Font color: Text 1